THE MECHANISM OF THE PROLONGED ACTION OF THE SINGLE-CHAIN INSULIN, 70-01

by

KELLEY CARR

Submitted in partial fulfillment of the requirements for the degree of

Master of Science

Department of Biochemistry

CASE WESTERN RESERVE UNIVERSITY

January, 2018

CASE WESTERN RESERVE UNIVERSITY

SCHOOL OF GRADUATE STUDIES

We hereby approve the thesis of

Kelley Carr

candidate for the degree of Master of Science

Committee Chair

Dr. William Merrick

Committee Member & Primary Mentor

Dr. Faramarz Ismail-Beigi

Committee Member

Dr. Martin Snider

Date of Defense

November 17, 2017

*We also certify that written approval has been obtained for any proprietary material contained therein.

Table of Contents

PAGE

List of Tables

PAGE

List of Figures

PAGE

Acknowledgments

I would first like to thank my thesis advisor, Dr. Ismail-Beigi for his unwavering support in my continued education, and for his invaluable guidance throughout this project: thank you. I would also like to express my gratitude to Dr. Michael Weiss, Dr. Nelson Phillips and the members of the Weiss lab for providing the insulins tested in this project. I would like to thank my committee members Dr. Snider, and Dr. Merrick for their guidance on my thesis. I would also like to thank my lab members for their immense help with experiments, this work could not have been completed without them: Homa Phillips, Alisar Tustan, Mamuni Swain, and Paul Macklis. Finally, I would like to thank all the people who mentored me and helped me develop the skills I have now: Nischay Rege, Michael Glidden, Dr. Yen-Shan Chen, and Parvin Hakimi. I owe my success to all of them.

I would also like to thank my husband, Clayton Carr who has sacrificed so much to support me through these last 3 years. Thank you for everything you have done so that I could stay focused. Thank you for helping me prepare for exams even though you were exhausted from a long day at work. But most importantly, thank you for your constant encouragement, and always reminding me I could do this.

List of Abbreviations

Asp	Aspartic Acid
BSA	Bovine Serum Albumin
BW	Body weight
Dil	Diluent
EC50	Half maximal effective concentration
ERK	Extracellular-signal Regulated Kinase
GIR	Glucose Infusion Rate
GLUT4	Glucose Transporter 4
HI	Human Insulin
His	Histidine
HRP	Horseradish Peroxidase
IRPY	Insulin Receptor Phosphorylated Tyrosine
IRS1	Insulin Receptor Substrate 1
IV	Intravenous
KP	Insulin *lispro*, Humalog
Lys	Lysine
PI3K	Phosphatidylinositol-4,5-bisphosphate 3-kinase
Pro	Proline
PVDF	Polyvinylidene Fluoride
SCI	Single-chain insulin
SDS	Sodium Dodecyl Sulfate
Shc	Src homology 2 domain containing protein
SQ	Subcutaneous
STZ	Streptozotocin
TBS	Tris Buffered Saline
Thr	Threonine

The Mechanism of the Prolonged Action of the Single-Chain Insulin, 70-01

Abstract

By

KELLEY CARR

Insulin plays a key role in metabolism. Insulin binds to its insulin receptors on insulin responsive cell surfaces and stimulates cellular uptake of glucose, turns on glycolysis and glycogen synthesis, inhibits gluconeogenesis and glycogenolysis in the liver, and stimulates triglyceride synthesis.

Previous research has shown that amino acid substitutions, deletions, or additions on insulin alter insulin function. We have found the single-chain insulin (SCI) 70-01, with a substitution of B10His to Asp (12,16), causes blood glucose to fall as rapidly as KP but remain lower longer when injected in diabetic rats. The focus of this research is to study the mechanism of 70-01's prolonged action, and compare it to control insulins, including 81-01, an identical SCI devoid of the AspB10 substitution.

We conclude that 70-01 remains for a longer period in the bloodstream, and continues to stimulate phosphorylation of the insulin receptors in a tissue-specific manner, longer than control insulins.

Introduction

Insulin is a hormone protein that is necessary for the regulation of many metabolic processes, including the uptake of glucose from the bloodstream into insulin sensitive tissues, lipid and protein metabolism, RNA and DNA synthesis, and cell growth (1,2,3,8). Insulin is synthesized in the beta cells of the pancreas and is released into the bloodstream by these cells in response to a rise in blood glucose levels (2). Insulin is clinically relevant due to the increase in prevalence of diabetes in the US: 29.1 million Americans were recorded as having diabetes in 2012, with 1.4 million being diagnosed every year (9). Diabetes has two forms, type 1 and type 2. Type 1, also called juvenile diabetes, is most often diagnosed at a young age. It occurs when the pancreatic beta cells undergo apoptosis under immunological attack and insulin production is markedly reduced (13). Type 2 diabetes occurs when the body becomes resistant to insulin. In response, beta cells produce more insulin to overcome the decreased insulin sensitivity to maintain near-normal euglycemia. Over years, insulin secretion decreases (in part due to beta cell death caused by endoplasmic reticulum stress) and glucose homeostasis is no longer maintained (2).

Insulin was first purified in 1921, but breakthroughs in the structure of the protein would not occur until 1954 when Sanger, et.al discovered its primary structure (4,5). The protein is 51 amino acid residues long and consists of two separate chains: the A chain and the B chain (Fig 1). The A chain is 21 residues in length and the B chain is 30 residues. The two chains are held in conformation by two inter-chain disulfide bridges which span the cysteine residue at position 7 of the A chain (A7) to the

Fig 1. Amino acid sequence of the primary structure of mature insulin. Disulphide bonds are also noted. Modified from figure provided by Nischay Rege.

cysteine residue at position 7 of the B chain (B7), as well as from A20 to B19. A third intra-chain disulfide bridge within the A chain spans from residues A6-A11 (3).

Proinsulin is a precursor to the mature hormone and has a C chain linker that connects the GlyA1 to the ThrB30 (Fig 2A). The 30-35 residue C chain is cleaved out in beta cells to produce the mature two chain hormone (Fig 2B; 3). Human proinsulin is more stable than the mature protein. When exposed to acidic pH and high temperature conditions, proinsulin resists fibrillation longer than two-chain wild-type insulin. The lag time of fibril formation is 15-fold longer than human insulin in the same conditions (17).

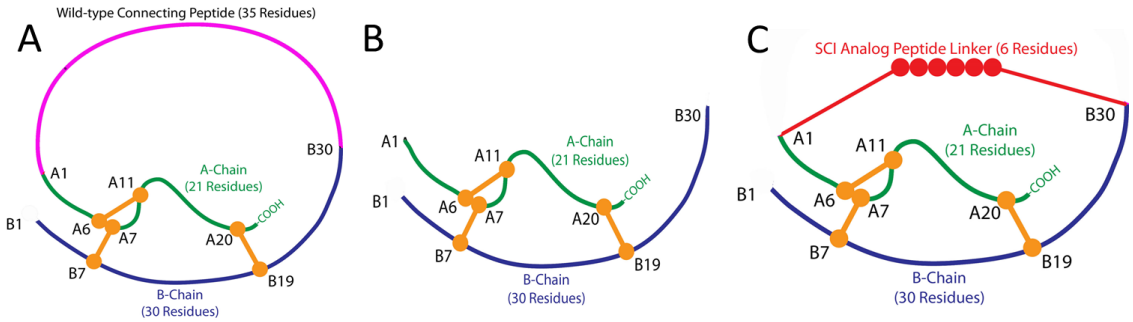

Fig 2. Diagram representation of proinsulin, mature insulin, and SCI's. Proinsulin **(A)** is represented as the B-chain (blue), A-chain (green), and the C-peptide linker (magenta). Mature insulin **(B)** is represented as the B-chain and A-chain held together by disulphide bonds (orange). The general structure of single-chain insulins (SCI's) **(C)** is represented as the A-chain and B-chain, and the 6 residue connecting linker (red). Modified from figure provided by Michael Glidden.

Insulin binds to the insulin receptor located on the cell surface. This receptor is a member of the tyrosine kinase superfamily (3). The insulin receptor is a heterotetrameric glycoprotein with two beta chains and two alpha chains (8). The chains

are held together by disulphide bonds and span the cellular membrane (8). The alpha chains are located entirely on the extracellular side of the membrane and are the location where insulin attaches. When insulin binds to the alpha chains, it causes a conformational change that brings the intracellular beta chains closer together and they autophosphorylate and trans-phosphorylate (6,8). Important tyrosine residues that are phosphorylated are Y972, Y1150, Y1158, Y1334, and Y1345, which may become phosphorylated to varying degrees (7). After phosphorylation, the insulin receptor is now active and creates a cascade of phosphorylation of signaling proteins affecting many cellular pathways including the Shc, Ras, and Erk pathways as well as the IRS1 and PI3kinase pathways (3,8). After signaling, the insulin receptor may become incorporated into clathrin-coated vesicles for internalization. These vesicles transport the complex to endosomes where the insulin is unbound and degraded in lysosomes, and the insulin receptor is either degraded or recycled to the cell surface (8). The phosphorylation of Y972 has been reported to play a role in internalization as well as signal transduction (8). The C-terminal tyrosines, Y1334 and Y1345, may reduce mitogenic activity (8).

Substituting amino acid residues on the insulin protein, or adding or deleting residues, can alter physiological properties of the insulin. For example, KP differs from wild-type human insulin in that the proline at B28 is switched with the lysine at B29 (10, 11). This seemingly minor transposition causes KP to be more rapid-acting than human insulin when injected subcutaneously (10). In wild-type human insulin, the proline residue at the B28 position functions in insulin dimer formation. These dimers then form hexamers around two zinc atoms. When injected subcutaneously, these hexamers

dissociate to dimers, and then to monomers for absorption into the bloodstream. This causes a delay in absorption and in removal of glucose from the bloodstream. When this proline is switched with the lysine at B29, the insulin molecules can only form very weak dimers, and very few hexamers. This allows for quick dissociation of the dimers or hexamers into monomers and, therefore, a more rapid absorption from the subcutaneous tissue into the bloodstream for a more rapid-acting insulin than human insulin (11). This understanding that the changing of amino acids can alter the effects of the protein substantially is the foundation for this project.

Based on the understanding that the single-chain nature of proinsulin increases the stability of the molecule compared to mature insulin, novel single-chain insulins (SCI's) have been engineered in Dr. Weiss's laboratory (12,16,17). Increased stability, especially in the event of increased temperatures, is a favorable property for clinically used injectable insulins and for insulins used in insulin pumps (16). Active SCI analogues contain a C-peptide linker of at least four amino acid residues connecting the A chain to the B chain, in a similar fashion to the C peptide of proinsulin (Fig 2C; 12). We have found that SCI's with two or less residues for the linker are not biologically active since they presumably hinder the protein from properly fitting into the binding site of the insulin receptor (12,16). 70-01 has a six amino acid linker of GGGPRR connecting the threonine residue at the B30 position with the glycine residue at the A1 position (Fig 2C; 12). In addition to the linker, 70-01 also has substitutions at A8 (Thr to His), B10 (His to Asp), B28 (Pro to Asp), and B29 (Lys to Pro). When injected into diabetic rats, 70-01 lowers blood glucose levels as rapidly as KP, but glucose levels remain lower for a much

longer period than KP. This study analyzes the mechanism for the prolonged action of the novel single-chain insulin 70-01. KP will be used as the clinical control insulin, and diluent will be used as the vehicle control. We will also use another SCI analog as a control, this analog named 81-01 contains the same amino acid substitutions and additions as 70-01, with one exception: 81-01 retains the native His at B10.

Previous reports have shown that human insulin (HI) mutated at position B10 to an Asp (instead of the normal His), labeled AspB10-HI, exhibits prolonged insulin signaling and is mitogenic (14, 15). 70-01, contains the AspB10 mutation and exhibits increased stability but surprisingly less mitogenicity compared to HI (16). The aim of the studies detailed below is to expand on previous research by examining this SCI's action and also to compare it to another identical SCI that is devoid of the AspB10 mutation, SCI 81-01. KP and diluent-injected diabetic and non-diabetic rats will be used as controls.

Experimental methods

Rats

Male Lewis rats weighing 250-300 gm were rendered diabetic by intraperitoneal injection of 48 mg/kg streptozotocin (STZ; MP Biomedicals). Diabetes was confirmed after 72 hour quarantine by blood glucose measurement of >250 mg/dL. A second injection of 48 mg/kg STZ was given if rats did not become diabetic after the first injection. Rats were used in experiments no longer than one year post stable induction of diabetes.

Pharmacodynamic studies

Insulins to be tested were injected subcutaneously or intravenously in diabetic rats. The subcutaneous injections were in the excess skin of the back of the neck in conscious rats. Intravenous injections were in the tail vein of the rat while the rat was anesthetized under isoflurane anesthesia. The tip of the tail was snipped and milked for a small blood sample in which blood glucose levels were measured via standard glucometers (EasyMax V). Blood glucose measurements were made every 10 minutes for the first hour, every 20 minutes for the second hour, 30 for the third hour, and then once per hour for the remainder of the experiment. A time course of the action profile of each insulin was created.

Additionally, a modification to this protocol for measuring plasma insulin levels was performed. This modification was performed in only a few experiments and entailed the rat being re-anesthetized briefly at 30, 60, 120, 240, and 360 minutes after intravenous injection, and blood samples were collected from the tail vein for measurement of plasma insulin levels.

Euglycemic clamps for measurement of plasma insulin half-life

Non-diabetic male Lewis rats were obtained from standard vendor with an exteriorized jugular catheter line already in place. Food was removed approximately four hours prior to the start of the experiment. Rats were briefly anesthetized with isoflurane and the jugular catheter was connected to infusion lines pre-filled with insulin, saline, and 35% glucose. The insulin was infused at a constant rate, and glucose

was infused at a variable rate to maintain euglycemia within 80 and 100 mg/dL. Solutions were infused using Harvard Apparatus programmable syringe pumps. After two hours, the insulin infusion was terminated and blood samples were obtained from a tail snip in the tip of the tail approximately every five minutes for a duration of 40 minutes. A variable infusion of 35% glucose was continued to maintain euglycemia while blood samples were obtained. Blood was collected in heparinized tubes, centrifuged, and plasma was collected and stored at -20°C until radioimmunoassays could be performed to measure plasma insulin concentrations for the determination of insulin half-life. In some experiments, a 3.07 nmol/ 300 gm body weight bolus of KP or 70-01 was administered subcutaneously, and glucose and saline were infused at variable rates to maintain euglycemia. Blood samples were obtained at 20, 40, 60, 80, 120, 180, 240, and 300 minutes after injection and plasma concentration was determined using radioimmunoassay. Euglycemic clamp protocols were modified from *Glucose Clamping the Conscious Mouse: A Laboratory Course*. Vanderbilt-National Institute of Diabetes and Digestive and Kidney Diseases Mouse Metabolic Phenotyping Center, University of Vanderbilt, Nashville, Tennessee (20).

Tissue Collection

12 diabetic Lewis rats in groups of three each were anesthetized and injected intravenously via the tail vein with 100 µl of Eli Lilly diluent (control), 2.56 nmol/ 300 gm body weight KP, or the SCI analogues 70-01 or 81-01, dissolved in 100 µl of the diluent. At time 0 and 20 minutes post-injection, blood glucose was measured. Rats were then decapitated under isoflurane anesthesia. Liver, epididymal

adipose tissue, quadriceps (a mixed-fiber-skeletal muscle), and heart ventricular muscle were immediately harvested and frozen on dry ice. The experiment was repeated on another day using 12 more diabetic rats except that tissues were harvested at 120 minutes post injection. All tissues were stored in a -80°C freezer for less than three months prior to assay.

Another experiment performed on two additional days had a similar design as this experiment, except rats were injected subcutaneously with 3.07 nmol/ 300 gm body weight KP or 70-01, or 100 µl/ 300 gm body weight diluent. These rats were sacrificed at 20 minutes and 30 minutes after injection (data at these time points were averaged together and labelled 25 minutes after injection), 240 minutes, or 360 minutes after injection. Liver and mixed quadriceps muscle tissue were collected and stored at -80°C. Blood samples were also collected and plasma insulin levels were measured.

Tissue Preparation

Tissues were homogenized in RIPA Lysis Buffer System (Santa Cruz Biotechnology Inc) prepared as per supplier's protocol. Additionally, Pierce protease inhibitor tablets and Pierce phosphatase inhibitor tablets (Thermo Fisher Scientific, Inc) were added to the lysis buffer at 2x concentration. All tissues were frozen when homogenized, and all procedures were performed on ice or in a cold room. 1000 µl Lysis buffer per 100 mg were added to liver tissue. Two 100 µl spoonfuls (spoon purchased from NextAdvance) of zirconium oxide 0.5 mm diameter beads were added to each sample. Samples were placed in the Bullet Blender Storm

(NextAdvance, Inc) tissue homogenizer on a setting of eight for five minutes, or until completely homogenized. Samples were centrifuged 10,000 x g for 10 minutes. Supernatants were removed and aliquoted to several Eppendorf microfuge tubes. Adipose tissue was homogenized as written above, except only 500 µl/ 100 mg tissue of lysis buffer was added.

Quadriceps muscle was homogenized in 700 µl/ 100 mg tissue RIPA lysis buffer system mentioned previously using the Fisher Scientific Laboratory Homogenizer, Model 125 with the FSH-G 7/107 generator. Samples were centrifuged at 17,000 x g for 10 minutes. Heart tissue was homogenized in a similar fashion except 1000 µl/ 100 mg tissue lysis buffer was added and the FSH-G 5/085 generator was used.

Protein concentrations were determined for each sample using the Pierce BCA protein assay kit (Thermo Fisher Scientific, Inc). The assay was performed as per the supplier's protocol for the microplate procedure. Absorbance at 562 nm was measured on the VersaMax Microplate reader.

Western Blot

Samples contained ~25 ug protein in 10 µl buffer. Approximately 4 µl of 4x Laemmli buffer (Bio-Rad) with 10% beta-mercaptoethanol was added to samples, heated at 50°C for 10 minutes for the samples to be probed for insulin receptor, and then centrifuged at 10,000 rpm for one minute. Samples to be probed for AKT were treated the same except heated at 100°C for five minutes. Samples were

loaded into Mini-PROTEAN TGX, 10%, 15-well, 15 µl gels (Bio-Rad), and run in 1x Tris/Glycine/SDS buffer at 85-90 V for approximately 2.5 hours.

Proteins were transferred to 0.2 µm PVDF membrane in 1x Tris/Glycine buffer and 20% methanol at 30-35 V for 1.5 hours. Membranes were washed three times with 1xTBS/0.1% Tween-20, and then blocked in 5% BSA or 10% non-fat milk for one hour. Membranes were washed three times with 1xTBS/0.1% Tween-20 and incubated overnight in 4°C cold room on a rocker in either Insulin Receptor β (Cell Signal), Phosphorylated-Insulin Receptor β (Tyr1150/1151) Rabbit mAb (Cell Signal), Phosphorylated-Insulin Receptor(Tyr1158) Polyclonal Antibody (Thermo Fisher Scientific), Phosphorylated-Insulin Receptor (Tyr1334) Polyclonal Antibody (Thermo Fisher Scientific), Phosphorylated-Insulin Receptor β (Tyr1345) Rabbit mAb (Cell Signal), Anti-Insulin Receptor (phosphorylated-Y972) antibody (Abcam), or a mixture of all five antibodies combined (labelled IRPY mix). Dilutions for all antibodies were 1:5000 in 5% BSA. Loading control was GAPDH diluted 1:10,000 in 10% non-fat milk. Additionally, AKT (Santa Cruz, Cell Signal) or phosphorylated-AKT antibodies (Ser473; Santa Cruz, Cell Signal) diluted 1:2000 and 1:200 (respectively) in 10% non-fat milk were also probed.

The following day, membranes were washed again with 1xTBS/0.1% Tween-20 and incubated in Goat Anti-Rabbit HRP conjugated secondary antibody diluted 1:10,000 in 5% BSA (or 10% non-fat milk) for one to two hours at room temperature on a rocker. Membranes were washed three times with 1xTBS/0.1% Tween-20 and

incubated in Luminata Crescendo Western HRP Substrate (EMD Millipore) for 45 seconds and developed.

Analyses

Data were calculated for statistical significance using ANOVA and student's t-test.

Results

Glucose Lowering Effect of 70-01 and 81-01

Fig 3 (pg. 28) shows the effect of these insulins (70-01, 81-01, and KP) or diluent on blood glucose levels of STZ-induced diabetic rats. 70-01 lowers blood glucose levels as quickly as the KP control for the first hour after subcutaneous injection, but 81-01 is slightly delayed (Fig 3A & 3B). The rate of fall for the first hour for KP was 278 ± 17.3 mg/dL/hour, the rate of fall for 70-01 was 317 ± 14.5 mg/dL/hour, and the rate of fall for 81-01 was 197 ± 10 mg/dL/hour ($p < 0.01$ compared to KP and 70-01). KP reaches a nadir of about 65% below baseline at 80 minutes post-subcutaneous injection, whereas 70-01 reaches a nadir of 80% below baseline at 100 minutes post-injection. 81-01 reaches its nadir of roughly 80% below baseline at 150 minutes post-injection. As blood glucose levels in KP and 81-01 injected rats begin to return to baseline, the blood glucose levels of rats injected with 70-01 plateau at roughly 80% lower than starting blood glucose levels. This plateau lasts at least six hours at a dose of 3.07 nmol/ 300 gm body weight (Fig 3A & 3B). These results indicate that 70-01 acts as a biphasic insulin, it exhibits rapid onset of action immediately after injection, as well as prolonged action (as in pre-mix insulins).

Next, insulins were injected intravenously (Fig 3C & 3D). Intravenous injections allow for the insulin to immediately enter blood circulation, whereas, when injected subcutaneously, the insulin must disperse and then diffuse through the subcutaneous space and into the bloodstream. Results following intravenous injection are similar to the subcutaneous injection, 70-01 has prolonged action compared to KP and 81-01, however, the duration of effect is slightly shorter at five hours at a dose of 1.54 nmol/ 300 gm body weight (Fig 3C & 3D). Also, 81-01 has a much faster rate of fall, tracking more closely with KP than when injected subcutaneously: KP's rate of fall for the first hour was 307 ± 18 mg/dL/hour, 81-01 was 256 ± 35 mg/dL/hour, and 70-01 had the slowest rate of fall at 224 ± 8 mg/dL/hour.

Effect of insulin response to different doses

To examine whether the prolonged action of 70-01 is dose dependent, we performed dose response experiments. STZ-induced diabetic rats were injected intravenously with doses ranging from 0.38-6.14 nmol/ 300 gm body weight of KP or 70-01 (Fig. 4A & 4B respectively; pg. 29). The data are represented as fraction of initial blood glucose vs time, i.e. the actual blood glucose at each time point divided by the initial blood glucose at time zero for their respective dose. At each dose, the effect of 70-01 lingers longer than the corresponding dose of KP. This indicates the long duration of action of 70-01 is not due to an overdose of the insulin. For example, note the difference using 3.07 or 0.77 nmol/ 300 gm body weight of the insulin compared to similar dose of KP.

Fig 5 (pg. 30) is another graphical representation of the dose response of KP to provide information on the dose at which maximum effect, or saturation of effect, is achieved. This graph shows the average decrease in blood glucose levels for the first hour for each dose. The EC50 for KP is approximately 0.77 nmol/ 300 gm, with a max effect reached at 3.07 nmol/ 300 gm.

Determination of plasma half-life of 70-01 and 81-01

To determine whether the prolonged action of 70-01 is in part due to a prolonged half-life, we conducted pharmacokinetic experiments in non-diabetic rats to determine the insulin's plasma half-life (Fig 6; pg. 31). In these studies, catheterized non-diabetic rats received a constant infusion of either KP, 70-01, or 81-01, and a variable rate of 35% glucose to maintain euglycemia (blood glucose levels between 80-100 mg/dL). After two hours, the insulin infusion was stopped and blood samples were obtained to measure plasma insulin concentrations. The fall in plasma insulin levels was calculated and used to determine the insulin half-life. The half-life of 70-01 and 81-01 were 17 ± 3 minutes and 22 ± 2 minutes respectively (not significantly different); however, both are significantly longer than KP at 8 ± 1 minute ($p < 0.05$).

Additionally, catheterized non-diabetic rats received a 3.07 nmol/ 300 gm body weight bolus injection of KP or 70-01 (Fig 7; pg. 32). Blood glucose was maintained between 90-110 mg/dL with a variable infusion of glucose and saline (Fig 7A). Blood samples were obtained every 20 minutes for the first two hours, then every hour up to five hours and were measured for plasma insulin concentration (Fig 7B). Rats injected

with 70-01 required higher glucose infusion rates (GIR) for longer to maintain euglycemia than rats injected with KP. Rats injected with the bolus of 70-01 were still dependent on a GIR of 10 mg/kg/minute five hours after injection to maintain euglycemia, whereas glucose infusion was stopped just after three hours for KP injected rats.

Plasma insulin concentrations for KP and 70-01 at 20 minutes after injection were 8 ng/ml and 18 ng/ml. KP was no longer measurable in the bloodstream after two to three hours, but 70-01 remained measureable in the bloodstream three to four hours after injection of the same dose of 3.07 nmol/ 300 gm body weight.

Determination of plasma insulin levels following bolus insulin injection

Tables 1 and 2 (pg. 33) show the concentration of plasma insulin in STZ-induced diabetic rats at specific times following intravenous or subcutaneous injections of 3.07 nmol/ 300 gm body weight KP or 70-01. At each time, blood samples were obtained and plasma insulin concentrations were measured. KP can be measured in the blood plasma up to 60 minutes after intravenous injection. 70-01 lingers quite a bit longer, up to 240 minutes after either subcutaneous injection or intravenous injection.

Analysis of Insulin receptor and AKT phosphorylation

Next, western blots were used to determine if the prolonged action profile of 70-01 is in part due to protracted signaling of insulin receptor or AKT. The phosphorylation state of the insulin receptor and AKT were measured in STZ-induced diabetic rats injected intravenously with 2.56 nmol/ 300 gm body weight KP, 70-01, 81-01 and 100

µl/ 300 gm vehicle control (Fig 9; pg. 35). On day one, 12 rats were injected and euthanized after 20 minutes. Blood glucose levels were measured to ensure successful injection (Fig 8; pg 34). Liver, skeletal (quadriceps) muscle, heart (ventricle), and epididymal adipose tissues were collected (Fig 9A & 9B). 12 more rats were injected on day two, but were euthanized after 120 minutes and the same tissues were harvested (Fig 9C & 9D). Liver, skeletal muscle, and adipose tissue showed ~2-fold, ~3 to 8-fold, and ~2-fold (respectively) increase in phosphorylation of the insulin receptor in the KP, 70-01, and 81-01 injected rats compared to diluent injected rats at 20 minutes (Fig 9A).

At 120 minutes after injection, KP, 70-01 and 81-01 injected rats continued to show increased phosphorylation of the insulin receptor in skeletal muscle, with a range of 2 to 11-fold increase over diluent. In 120 minute heart muscle tissue, only 70-01 injected rats continued to show increased phosphorylation of about 2-fold increase over diluent. The signal ceased in both liver and adipose tissue samples at 120 minutes post-injection (Fig 9C).

Next, we looked at AKT, a molecule located further downstream in the insulin signaling pathway, to determine if protracted signaling of this molecule might contribute to the long-acting nature of 70-01 (Fig 9B & 9D). Western blot data of phosphorylated AKT shows strong signaling in heart (~8 to 10-fold increase) and adipose tissues (~2 to 3-fold increase) at 20 minutes for all three insulins, although the results in adipose tissue are not statistically significant. The skeletal muscle appears to be trending toward increased phosphorylation of AKT in all three insulins compared to diluent;

however, only 70-01 stimulated phosphorylation is statistically significant at 20 minutes. Liver does not have any AKT signaling at 20 minutes.

Interestingly, we see continued phosphorylation of AKT in the tissues collected after 120 minutes post-injection for KP, 70-01, and 81-01 in the skeletal muscle tissues (~8 to 10-fold increase over diluent). In heart muscle, KP stimulated phosphorylation of AKT is ~5-fold over diluent, but both 81-01 and 70-01 stimulated phosphorylation of AKT remain significantly higher at 6.5 to 8-fold compared to diluent. Again, there is no statistically significant phosphorylation in the liver tissue at 120 min (Fig 9D). Finally, 70-01 also continues to induce phosphorylation of AKT in the adipose tissue about 2-fold higher than diluent and KP, with a $p < 0.05$.

We also performed preliminary experiments to investigate the time course of action for KP and 70-01. In these experiments, the experimental design is similar to the previously described protocol, except rats were injected subcutaneously with diluent, or 3.07 nmol/ 300 gm body weight KP or 70-01 (Fig 10; pg. 37). For the first day of the experiment, rats were sacrificed at 30 minutes or 240 minutes after injection. On the second day, rats were sacrificed at 20 minutes or 360 minutes after injection. The 20 minute and 30 minute time point data were very similar, and due to this similarity, we averaged the two time points together and labelled the composite time point 25 minutes. These data are very preliminary and have a small n, and do not include data for insulin 81-01. Fig 11A (pg. 38) shows the fold change over diluent of phosphorylated AKT in the liver at 25 minutes, 240 minutes and 360 minutes. At 25 minutes, both KP (~ 2.5-

fold increase) and 70-01 (~2-fold increase) are statistically higher than diluent. This signal diminishes 240 minutes and 360 minutes after injection.

Figure 11B shows the fold change over diluent of phosphorylated AKT in the mixed (quadriceps) muscle. The muscle tissue from KP injected rats collected at 25 minutes has about 3.5-fold increase in AKT phosphorylation over diluent injected rats, and 70-01 is about 2-fold compared to diluent, but does not reach statistical significance. 70-01 induced phosphorylation does reach statistical significance in the 240 minute mixed muscle samples, whereas KP induced phosphorylation is diminishing. Both insulins appear to be finished signaling in the 360 minute mixed muscle tissues. Heart tissue was not collected for these experiments, and epididymal adipose tissue was discovered to be contaminated with vesicles and, therefore, was not analyzed.

Additionally, the 30 minute and 240 minute liver and mixed muscle samples were analyzed for phosphorylated tyrosine residues on the insulin receptor (Fig 12; pg. 39). In the liver, both KP and 70-01 stimulated phosphorylation are significantly higher than diluent at 30 minutes. Both lose significance in the 240 minute samples. In the muscle tissue, neither time point shows significance. This is most likely due to the small sample size.

Analysis of individual phosphorylated tyrosine residues on the insulin receptor

Next, we performed western blots on the tissues collected at 20 minutes and 120 minutes, but probed for phosphorylated tyrosine residues Y972, 1150, 1158, 1334, and 1345 located on the beta chain of the insulin receptor (Figs 13-16; pg. 40-47). Each

of these graphs includes the total phosphorylated tyrosine data that was shown in Fig 9 for reference. This data is labelled IRPY mix to designate the membranes were probed with a mixture of all five phosphorylated tyrosine residue antibodies.

At 20 minutes, the liver tissue shows statistically significant signaling of tyrosine residues 1150 and 1158 in 70-01 and 81-01 treated rats, but no difference in residues 1334, 1345, or 972. All signaling is diminished in the 120 minute liver samples for all tyrosine residues (Fig 13).

For the mixed muscle, tyrosine residues 1150, 1158 and 1334 all show statistically significant stimulation at 20 minutes (Fig 14). This signaling becomes further augmented in 70-01 for Y1150 (15-fold increase) and both 70-01 and 81-01 for Y1158 and Y1334 in the 120 minute mixed muscle samples. Interestingly, the total phosphorylated tyrosine mixture does not show statistically significant phosphorylation in the 20 minute samples, but does show statistical significance in the 120 minute samples. Just like the liver samples, Y1345 and Y972 show no activity.

Unlike the mixed muscle, the heart shows very little to no phosphorylation of the insulin receptor (Fig 15). Only 81-01 in tyrosine 1150 is statistically significant. The 120 minute heart tissues do not have significance for the individual tyrosine residues; however, 70-01 achieves significance when all five phosphorylated tyrosine antibodies are mixed together.

The 20 minute adipose tissues have no statistically significant phosphorylation of the tyrosine residues compared to diluent (Fig 16). When all five tyrosines are mixed

together, KP, 70-01, and 81-01 injected rat adipose tissues show approximately a 2-fold increase in insulin receptor tyrosine residue phosphorylation over diluent, which is statistically significant. The phosphorylation is lost in the 120 minute adipose tissue samples.

Conclusion

Proinsulin, the single-chain precursor to the mature hormone insulin, has been shown to be more stable when exposed to low pH or high temperatures than the two-chain mature hormone (17). This concept of a single-chain molecule having increased stability compared to two-chain insulin led to the development of the single-chain insulin 70-01 (12,16). When injected in STZ-induced diabetic rats, 70-01 was found to lower blood glucose levels as fast as control insulins, and maintain lower blood glucose levels much longer than controls. We sought to better understand the mechanisms behind this unusually fast-acting and long-lasting insulin. In this project, we compared 70-01 to KP, 81-01, and diluent. KP is a well researched two-chain insulin currently being used clinically as a rapid-acting insulin (11). Like 70-01, 81-01 is also a single-chain insulin, and has the same modifications as 70-01 except it is devoid of the AspB10 mutation. Therefore, we used 81-01 as a control for the AspB10 mutation in 70-01. AspB10 is known as a mitogenic inducing mutation. Human insulin containing this mutation, as well as AspB10-KP, have increased affinity for the insulin receptor, which extends the signaling cascade and can lead to uncontrolled cell growth (11,15). Diluent was used as the vehicle control.

As seen in Fig 3A & 3B, 81-01 also has a longer duration of action than KP control when injected subcutaneously, but not as long as 70-01. Interestingly, 81-01 has a similar glucose-lowering effect as KP when injected intravenously. This suggests absorption of 81-01 from the subcutaneous space and diffusion into the bloodstream is delayed compared to KP or 70-01 when injected subcutaneously. This is further supported by the rates of fall in blood glucose levels for the first hour when injected subcutaneously. The rate of fall for the first hour for 81-01 was significantly lower than KP or 70-01.

Next, a dose response experiment was performed using KP and 70-01 to determine if the longevity of 70-01 was dose dependent. Our aims are to determine the mechanisms behind 70-01's longevity, overdose of the insulin must be ruled out as a possible explanation. Fig 4 shows the same dose of 70-01 is longer acting when compared to its respective dose of KP. This supports the single-chain insulin is innately longer acting than KP control, and cannot be explained by an overdose.

Next, we determined the half-lives of KP, 70-01 and 81-01 to examine the possibility that the prolonged action of these insulins may be related to a longer half-life. Our data are partially in support of this possibility. Both 70-01 and 81-01 have longer plasma half-lives compared to KP when infused intravenously. When insulin attaches to the insulin receptor, it activates a cascade of signaling and is then (along with the insulin receptor) engulfed into the cell and destroyed in lysosomes (8). Circulating plasma insulin levels decrease as the insulin attaches to insulin receptors and are destroyed. This data suggests that 70-01 is indeed attaching to and activating insulin

receptors, but is somehow released back into the bloodstream before it is destroyed. Alternatively, the insulin may remain within the cell and activate insulin receptors, which has been suggested previously for AspB10-KP insulin (15). However, this latter explanation implies high cellular residence of the insulin, and would not explain how plasma insulin levels for 70-01 remain so high. Never-the-less, one 70-01 insulin molecule may be able to activate many insulin receptors over a longer period of time than KP before it is degraded in the lysosome. Interestingly, 81-01 has a similar pharmacodynamic profile as KP when injected intravenously, but has a similar pharmacokinetic profile to 70-01 in that it has a long half-life.

Table 1 and 2 also show 70-01 remains in the bloodstream much longer than KP when injected subcutaneously or intravenously. Also worth noting, the 30 minute plasma insulin level measurements are very different, 70-01 is much higher than KP even though rats were injected with the same dose (moles) of either insulin. This same anomaly is seen in Fig 7B, plasma insulin levels of 70-01 are much higher 20 minutes after injection of the same dose (moles) than KP. This further supports the theory that 70-01 somehow avoids degradation and is consistent with its longer plasma half-life than KP.

Next we performed western blot experiments to analyze the phosphorylation events of the insulin receptor as well as AKT, a molecule located more downstream in the insulin signaling cascade. This molecule activates protein synthesis, induces cellular glucose uptake, inhibits apoptosis, and regulates glucose and lipid homeostasis (19). AKT is phosphorylated along a cascade of signaling that occurs after the insulin receptor

autophosphorylates itself in response to an insulin molecule attaching to the active site on the alpha subunit of the insulin receptor (8).

We hypothesized tissues harvested from 70-01 treated rats would show higher phosphorylation in insulin receptor and AKT than control and KP-treated rats, especially at later time points, and that 81-01 treated rats would show similar phosphorylation as the KP-treated rats, since these were intravenous injections. Liver, skeletal muscle and adipose tissue show positive phosphorylation of the insulin receptor at 20 minutes in insulin-treated rats, and positive phosphorylation of AKT in skeletal muscle, heart and adipose tissue at 20 minutes in insulin-treated rats (Fig 9B). Notably, insulin receptor phosphorylation of liver in 81-01 treated rats at 20 minutes are statistically higher than KP-treated rat livers at this time point (Fig 9A).

The results are somewhat consistent with our hypothesis for the insulin receptor phosphorylation 120 minutes after phosphorylation. 70-01 treated rats have statistically higher tyrosine phosphorylation on the insulin receptor in both skeletal muscle samples and heart samples, but not in the liver and adipose tissue (Fig 9C). For AKT phosphorylation 120 minutes after injection, skeletal muscle, heart and adipose tissue all have varying intensities of phosphorylation for all insulins (Fig 9D). With so much activity in the 120 minute group, it is possible the study design was flawed in that we did not pick a late enough time point to truly compare phosphorylation events of 70-01 to controls. This hypothesis is supported by Fig 8, which clearly indicates the blood glucose levels of the rats injected with KP, 70-01 and 81-01 are still much lower than diluent injected rats after 120 minutes. The time points of sacrifice chosen were 20 minutes and

120 minutes because blood glucose levels of rats injected with these test insulins in previous experiments (Fig 3C & 3D) are actively and rapidly falling at 20 minutes, and blood glucose levels of KP and 81-01 injected rats are beginning to rise back up to baseline at 120 minutes. Our prediction was that the 20 minute samples should give positive phosphorylation, and 120 minute samples may or may not give positive phosphorylation, but should certainly be less than rats treated with 70-01.

In light of these results, we performed preliminary experiments comparing 70-01 and KP at later time points (Fig 11). Please note these data points have a low n, do not compare 81-01, and were tested in a slightly different model: insulins were injected subcutaneously instead of intravenously. Nevertheless, some observations can be made from the data. First, there is successful phosphorylation of AKT in both the liver and mixed muscle tissues after 25 minutes. Secondly, all phosphorylation of AKT is dissipated in the liver at later time points. Thirdly, AKT phosphorylation in the mixed muscle tissue of 70-01 injected rats is significantly higher than KP at 240 minutes after injection, but not 360 minutes. According to tables 1 and 2, 70-01 is measurable in the bloodstream at 240 minutes after injection, therefore, 70-01 is somehow targeting the insulin receptors of mixed muscle tissue, but loses activity six hours after injection. Fig 12 shows insulin receptor phosphorylation of liver and mixed muscle but only at 30 minutes and 240 minutes after injection. Only 30 minute liver samples have statistically significant phosphorylation of the insulin receptor. The lack of statistical significance for the remaining data sets could be attributed to the small sample size.

Finally, we investigated the phosphorylation of specific tyrosine residues on the insulin receptor to determine differences between each tyrosine, and if these differences are tissue dependent or insulin dependent or both (Fig 13-16). The tyrosine residues are phosphorylated tyrosines 972, 1150, 1158, 1334, and 1345. Y972 is located on the beta chain of the insulin receptor close to the inner cellular membrane surface. This residue is located in the region of the insulin receptor designated the juxtamembrane region (7,8,18). Y972 is found in the NPEY motif, which is considered to be important for internalization of the insulin-insulin receptor complex. It is also important in signal transduction by acting as a recruitment site for signaling proteins (8,18).

Y1150 and Y1158 are located in the region of the beta chain called the catalytic kinase domain (7,18). This region is important for autophosphorylation and phosphorylation of substrates that begin the cascade of phosphorylation events (8,18). In studies in which these residues are replaced with phenylalanine, kinase activity is reduced, and the effect of insulin on cellular processes is diminished (8).

Y1334 and Y1345 are in the C-terminus region of the insulin receptor's beta chain and are implicated to be involved in the ability for the insulin receptor to undergo a conformational change upon ligand binding (8). This conformational change is necessary for the beta chains to move within reach of each other's kinase domains for autophosphorylation (8). Additionally, studies have shown the C-terminus region is involved in inhibiting mitogenic signaling. When tyrosines in the C-terminal domain are replaced with phenylalanine, mitogenic related signaling increases (8). All three domains

are also important attachment points for proteins involved in downstream signaling such as IRS-1, PI3K, APS and Shc (7,8).

Y1150 and Y1158 show higher phosphorylation in liver tissue of 70-01 and 81-01 injected rats after 20 minutes (Fig 13). This indicates the insulin receptors in the liver are catalytically active since these residues are in the kinase domain. The lack of phosphorylation in Y1334, Y1345, and Y972, as well as all tyrosines at the later time point suggest the insulins affect the liver in a time-sensitive manner. Perhaps tissue collected at shorter time points such as 5 or 10 minutes after injection would show much higher phosphorylation, especially in the KP samples as this insulin is a rapid, but short-acting insulin.

Mixed muscle samples have strong phosphorylation in Y1150, Y1158, & Y1334 after 20 minutes for KP, 70-01 and 81-01 treated samples, but even stronger phosphorylation at 120 minutes for 70-01 and 81-01. This suggests 70-01 targets muscle tissue. If 70-01 continues to signal all skeletal muscle surface Glut 4 receptors, a large amount of glucose will be removed from the bloodstream. This contributes to 70-01's ability to maintain blood glucose levels at 80% below baseline for many hours, as we have observed in Fig 3. In addition, Fig 3A & 3B show blood glucose levels in 70-01 injected rats remain plateaued from time 120 minutes, until 360 minutes and maybe beyond. Perhaps the liver has begun producing glucose via glycogenolysis or gluconeogenesis and releasing it in the bloodstream at a rate equal to what is being removed by the muscle tissue to counteract the low blood glucose levels.

This work has a few limitations. The first limitation is we had to switch suppliers for the AKT primary antibody in the middle of the studies as the original supplier stopped producing the antibody. We chose an antibody from an alternative supplier that was reported to be very similar to our original antibody. However, we did notice differences in signaling between the two antibodies. This may have contributed to the size of the error bars in some of the AKT data. The second limitation is the small n for the 240 and 360 minute data following subcutaneous injection of the insulins, as well as having no data for insulin 8101 at these time points.

Future work should expand on the time scale of these insulins injected subcutaneously and intravenously. The work in this study primarily examined insulin effects on AKT and insulin receptor phosphorylation in tissues collected at 20 minutes and 120 minutes after an intravenous injection. A few samples were analyzed from 25 minutes, 240 minutes and 360 minutes after a subcutaneous injection, but these data points have a small n. Experiments should be performed to increase the n for the 240 minute and 360 minute time points, as well as adding additional time points such as 60 minutes, 120 minutes, and 180 minutes after a subcutaneous injection. Additional time points following an intravenous injection should also be studied. These time points could include 60, 120, 180, 240 and 360 minutes. This model can also be used to test other novel insulin analogs created in Dr. Weiss' laboratory. These insulins could also be tested using the hyperinsulinemic euglycemic clamp experimental model which uses radioactivity to measure triglyceride synthesis, glycogen synthesis, and glucose uptake in liver, mixed muscle and adipose tissue of non-diabetic rats.

Here we offer a potential explanation for the prolonged glucose lowering effect of 70-01. Because there is no food intake during the prolonged experiment following the injection of 70-01, any increase in blood glucose level is potentially mediated by an increase in glucose delivery to the bloodstream by the liver (and to some extent, the kidney). The absence of insulin receptor or AKT phosphorylation in the liver at the longer time points would be consistent with this premise and may suggest that glucose production has increased. However, we note that during this period, glucose levels remain low. This leads to the conclusion that, even if glucose production is increased, glucose disposal mostly by muscle uptake is dominant. This premise is consistent with our finding of prolonged insulin receptor and AKT phosphorylation in skeletal muscle.

In conclusion, the single-chain insulin 70-01 may be a clinically relevant insulin. At late time points, if 70-01 is signaling glucose uptake in muscle tissue, while the diminished suppression of gluconeogenesis and glycogenolysis in the liver is preventing hypoglycemia, we may have discovered a basal insulin that will induce few to no hypoglycemic episodes, and may control blood sugar levels at a relatively euglycemic level between meals. Additionally, if the liver is producing glucose from glycerol via gluconeogenesis, we may have discovered an insulin that will stimulate fatty acid oxidation instead of fatty acid synthesis, which would alleviate the side effect of weight gain induced by injectable insulin use that plagues the use of insulins for treatment of type 2 diabetes today (21).

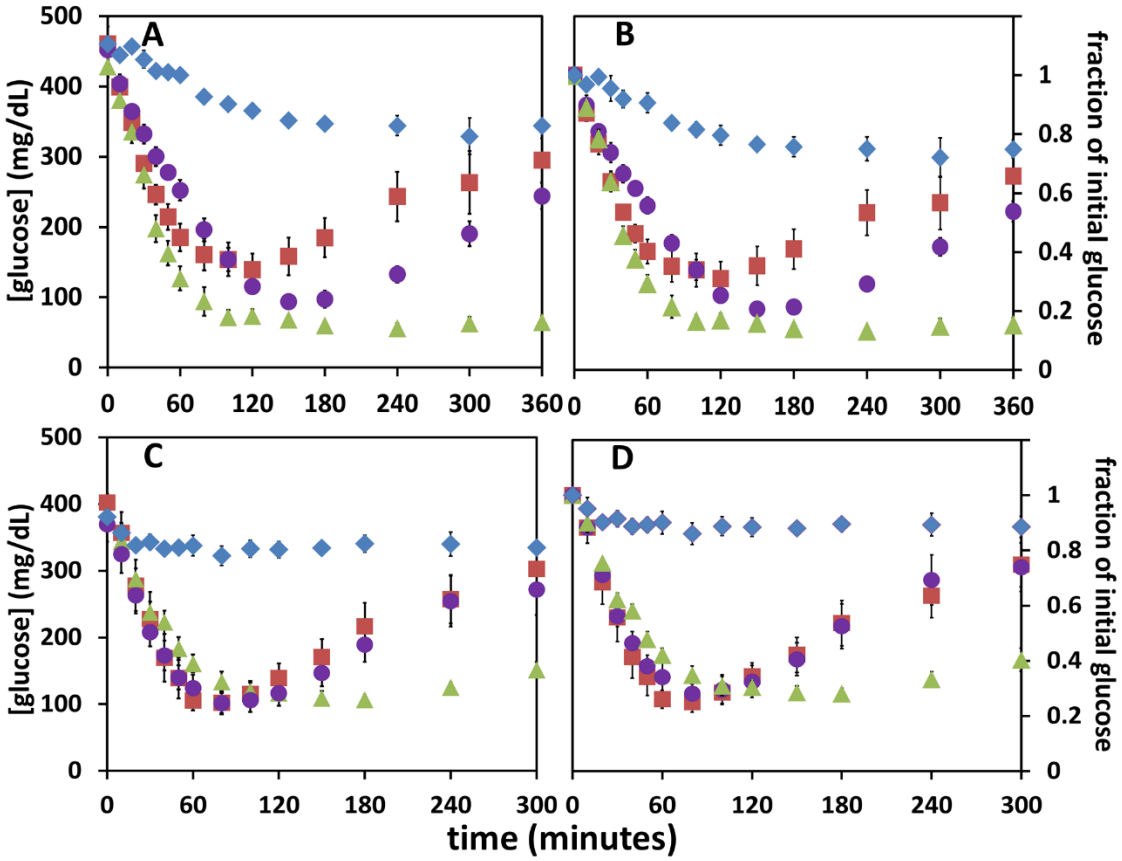

Fig 3. **Glucose-lowering effect of KP vs 70-01 vs 81-01.** Blood glucose measurements (mg/dL) over time of STZ-induced diabetic rats following a subcutaneous injection of 3.07 nmol/300 gm body weight (**A** & **B**) or an intravenous injection of 1.54 nmol/ 300 gm body weight (**C** & **D**) of KP (red square), 70-01 (green triangle), 81-01 (purple circle) or 100 µl/ 300 gm diluent (blue diamond). n= 5 to 7; mean ± SE.

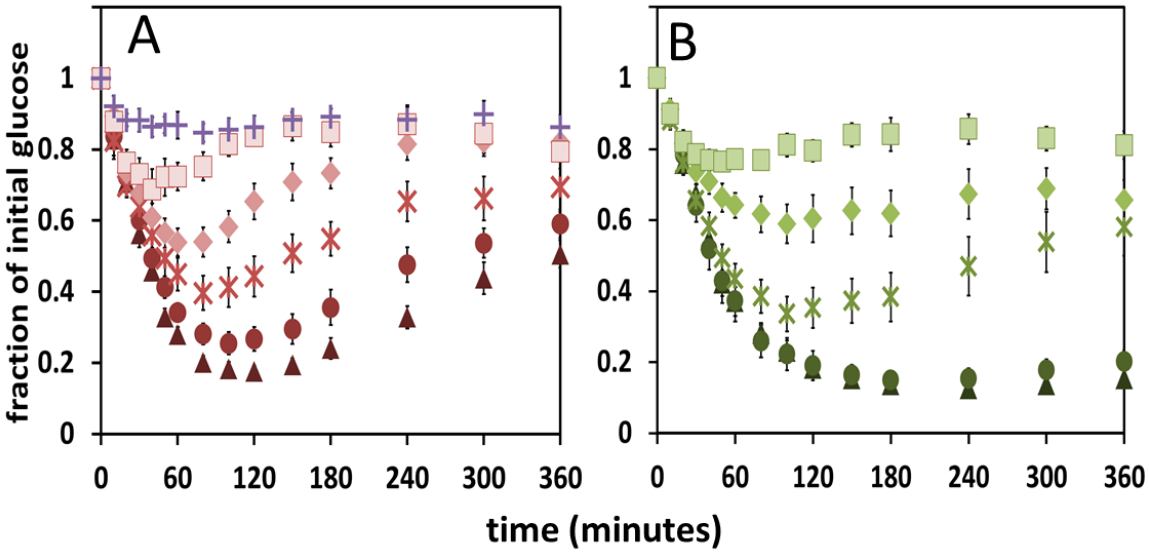

Fig 4. Fraction of initial blood glucose vs time in STZ-induced diabetic rats injected intravenously with variable doses of KP (**A**) or 70-01 (**B**). Rats received either 6.14 (triangle), 3.07 (circle), 1.54 (cross), 0.77 (diamond), 0.38 (square) nmol/ 300 gm body weight, or 100 µl/ 300 gm body weight diluent (plus sign). Initial blood glucose levels averaged 450 mg/dL. n=8 to 17; mean ± SE.

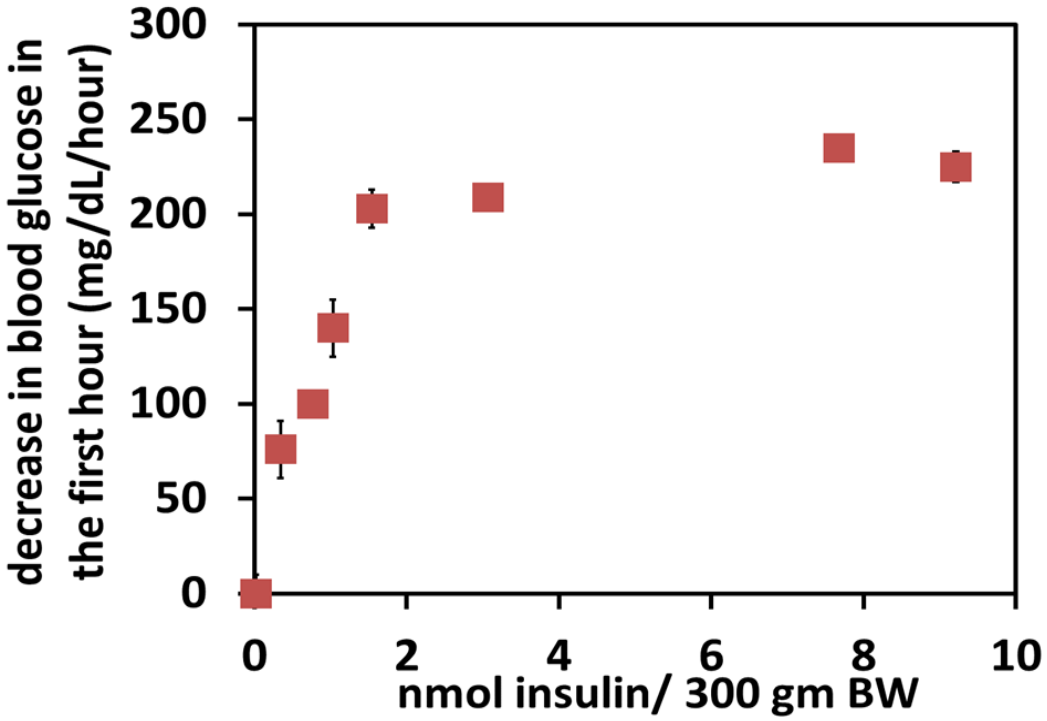

Fig 5. Dose response curve of KP. Graphical representation of the rates of fall during the first hour (mg/dL/hour) after subcutaneous injection of variable doses of KP. The following number of rats were used at each dose: Diluent n=20; 0.34 nmol n=7; 0.77 nmol n=35; 1.03 nmol n=7; 1.54 nmol n=14; 3.07 nmol n=30; 7.68 nmol n=35; 9.21 nmol n=15. Mean ± SE.

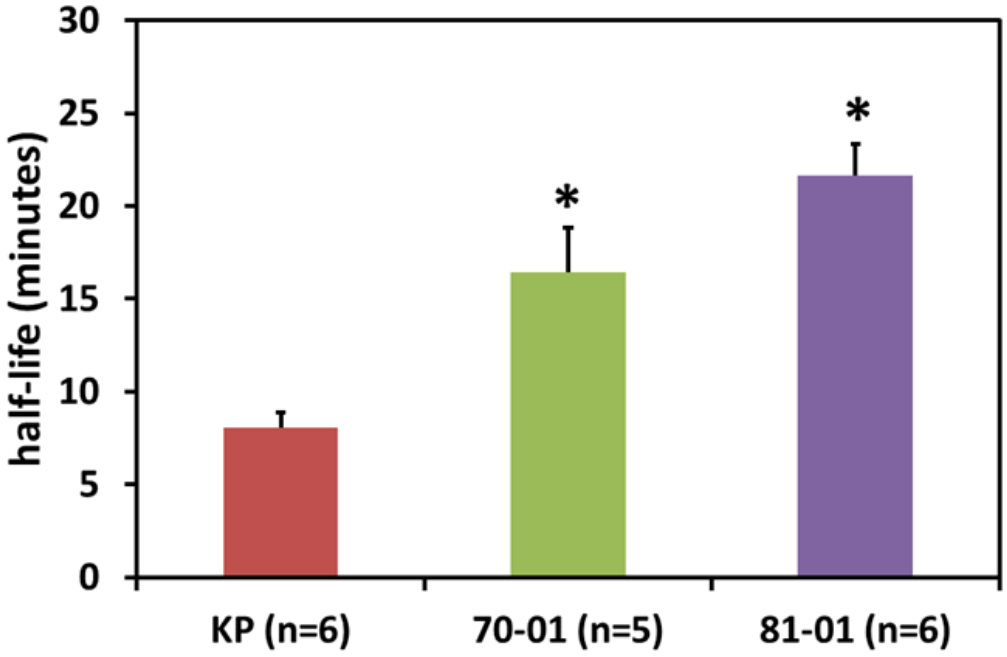

Fig 6. Insulin plasma half-life data. Non-diabetic rats were infused with 10 mU of insulin/kg/minute for 2 hours and glucose was infused to maintain euglycemia. After 2 hours the insulin infusion was terminated and blood was obtained at 5 minute intervals up to 40 minutes for determination of plasma half-life. mean ± SE. *denotes $p<0.05$ compared to KP. Thank you Alisar Tustan, Paul Macklis, and Homa Phillips for performing the experiments and calculating the data.

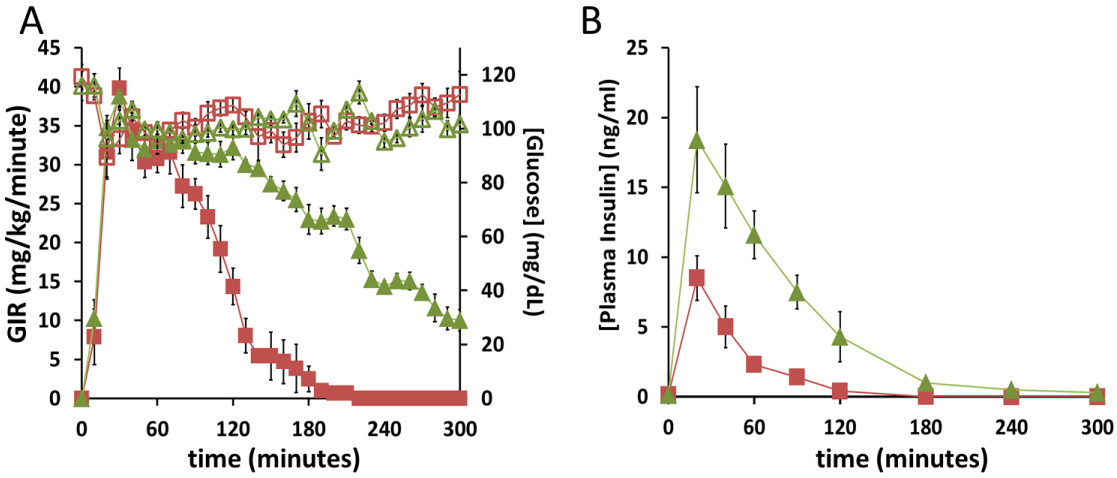

Fig 7. Pharmacokinetics and pharmacodynamics of KP vs 70-01. Experiments performed in catheterized non-diabetic rats. Rats received a subcutaneous bolus of 3.07 nmol/ 300 gm body weight of either KP (red squares) or 70-01 (green triangles), and a continuous infusion of glucose. Panel **A** represents the Glucose Infusion Rate (GIR; solid red squares for KP; solid green triangles for 70-01) in mg/kg/minute required to maintain euglycemia (the hollow squares for KP and the hollow triangles for 70-01). At specified time points, blood samples were obtained and analyzed by radio-immunoassay for plasma insulin levels (panel **B**). The red squares represent KP and the green triangles 70-01. n=6; mean ± SE. Thank you to Alisar Tustan and Homa Phillips for performing these assays.

IV Injection
3.07 nmol/ 300
gm

Minutes	30 (n=2)	60 (n=2)	120 (n=2)	240 (n=2)	360 (n=2)
[KP] (ng/ml)	5.88	2.01	0	0	0
[70-01] (ng/ml)	18	13.5	2.65	0.65	0

Table 1: Plasma insulin levels in ng/ml of KP and 70-01. Rats were anesthetized and 3.07 nmol/ 300 gm body weight insulin was injected intravenously. At each time point, rats were re-anesthetized and plasma samples were obtained from the tail vein for measurement of insulin concentration. Thank you Homa Phillips for measuring the insulin concentrations.

SQ Injection 3.07
nmol/ 300 gm

Minutes	25 (n=5)	240 (n=3)	360 (n=2)
[KP] (ng/ml)	7.94 (±1.82)	0	0
[70-01] (ng/ml)	28 (±3.69)	0.9	0

Table 2: Plasma insulin levels in ng/ml of KP and 70-01. Rats were injected subcutaneously with 3.07 nmol/ 300 gm body weight insulin. For these experiments, at the specified time points, rats were euthanized and plasma samples were collected for measurement of insulin concentration. Thank you Homa Phillips for measuring the insulin concentrations

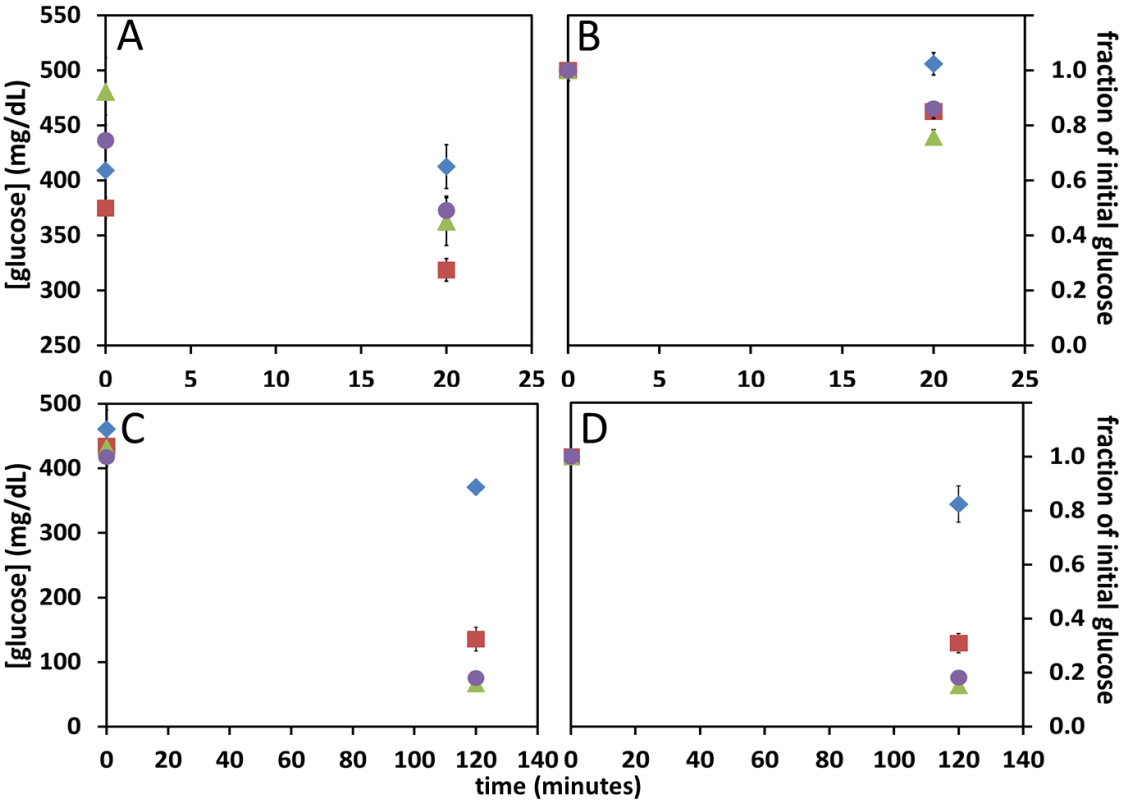

Fig 8. Fall in blood glucose levels in rats to be sacrificed for tissue collection experiments. STZ-induced diabetic rats were injected intravenously with diluent (blue), or 2.56 nmol/ 300 gm body weight of KP (red), 70-01 (green) or 81-01 (purple) all in 100 µl diluent. Rats were sacrificed at either 20 minutes (**A** & **B**) or 120 minutes (**C** & **D**) and liver, skeletal (quadriceps) muscle, heart (ventricle), and epididymal adipose tissue were harvested. n=6; mean ± SE.

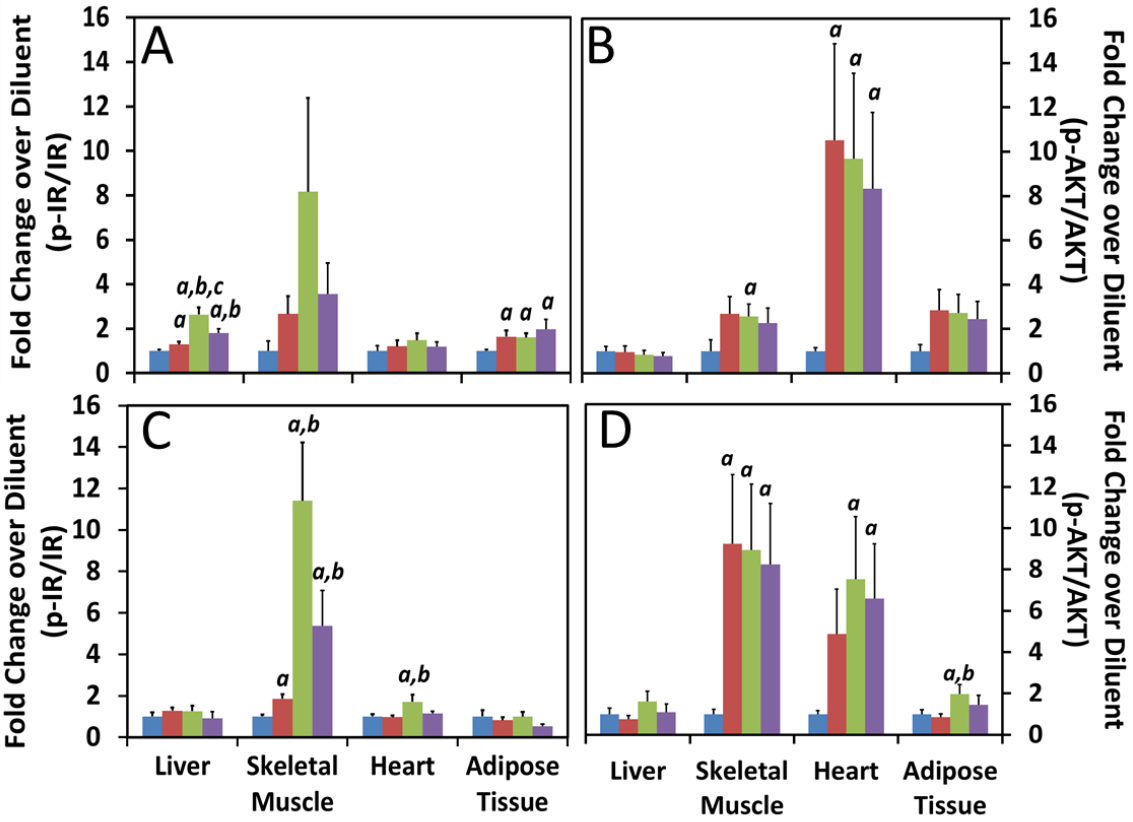

Fig 9. Effect of KP, 70-01, & 81-01 insulin on phosphorylation of IR and AKT in various tissue of the rat. Western blot data representing the fold change over diluent of tyrosine phosphorylated insulin receptor (**A** & **C**) and phosphorylated AKT (**B** & **D**)**.** STZ-induced diabetic rats were injected with diluent (blue), or 2.56 nmol/ 300 gm body weight of KP (red), 70-01 (green) or 81-01 (purple) all in 100 µl diluent. Rats were sacrificed at either 20 minutes (**A** & **B**) or 120 minutes (**C** & **D**) and liver, skeletal (quadriceps) muscle, heart (ventricle), and epididymal adipose tissue were harvested. n=6; mean ± SE ^{a} indicates $p < 0.05$ compared to diluent; ^{b} indicates $p < 0.05$ compared to KP; ^{c} indicates $p < 0.05$ compared to 81-01.

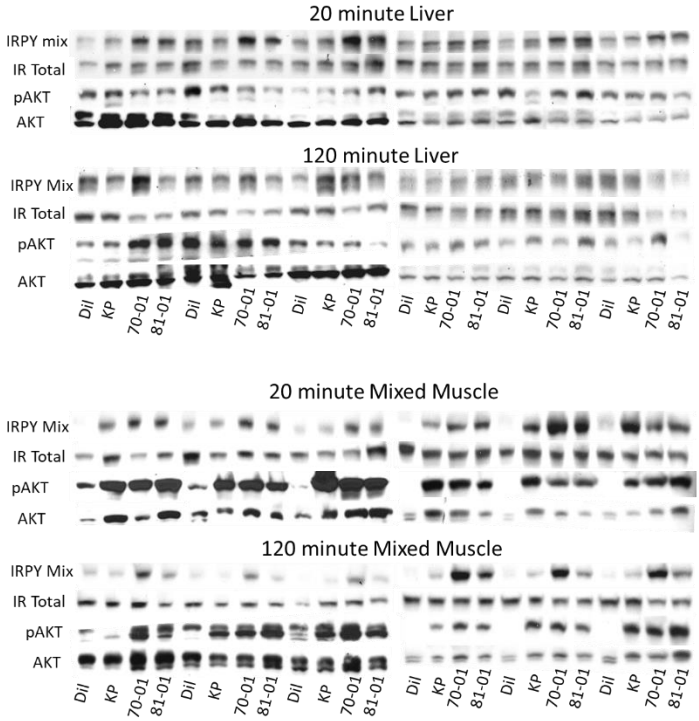

Fig 9-1. Western blots of phosphorylated insulin receptor (IRPY mix) and AKT in liver and mixed muscle.

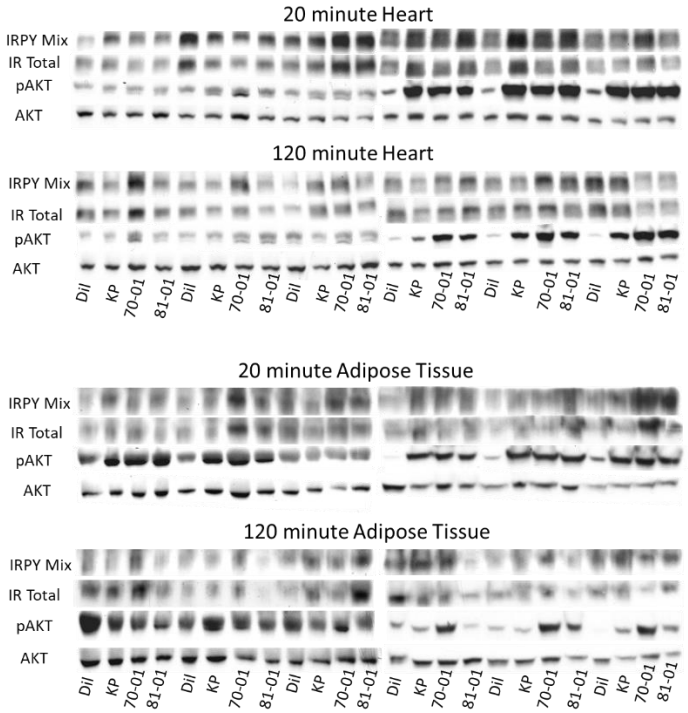

Fig 9-2. Western blots of phosphorylated insulin receptor (IRPY mix) and AKT in heart and adipose tissue.

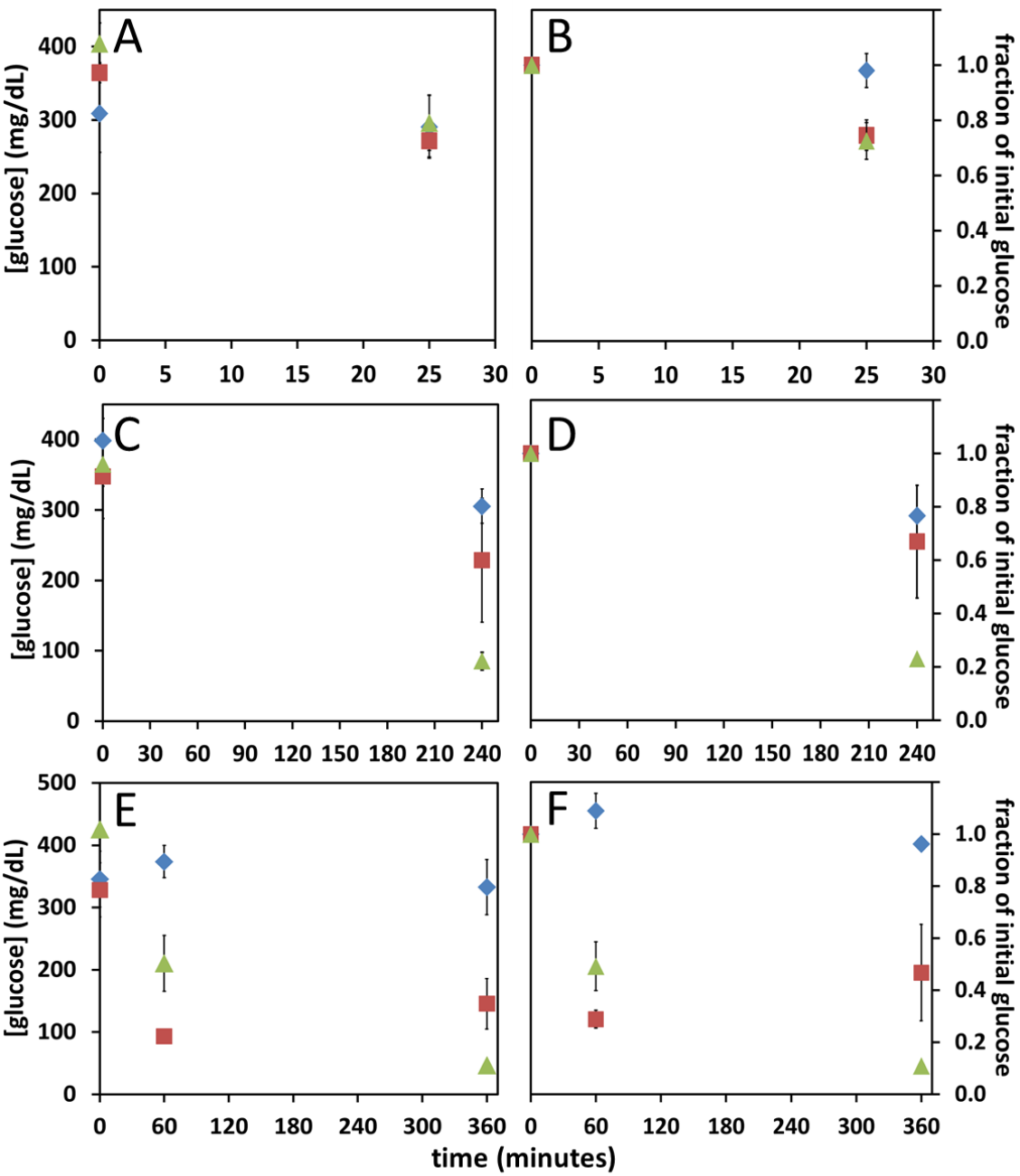

Fig 10. Fall in blood glucose levels in rats to be sacrificed for tissue collection experiments. STZ-induced diabetic rats were injected subcutaneously with diluent (blue), or 3.07 nmol/ 300 gm body weight of KP (red), or 70-01 (green) all in 100 µl diluent. Rats were sacrificed at either 25 minutes (**A & B**), 240 minutes (**C & D**), or 360 minutes (**E & F**) after injection and liver and mixed (quadriceps) muscle were collected. n = 2 to 5; mean ± SE.

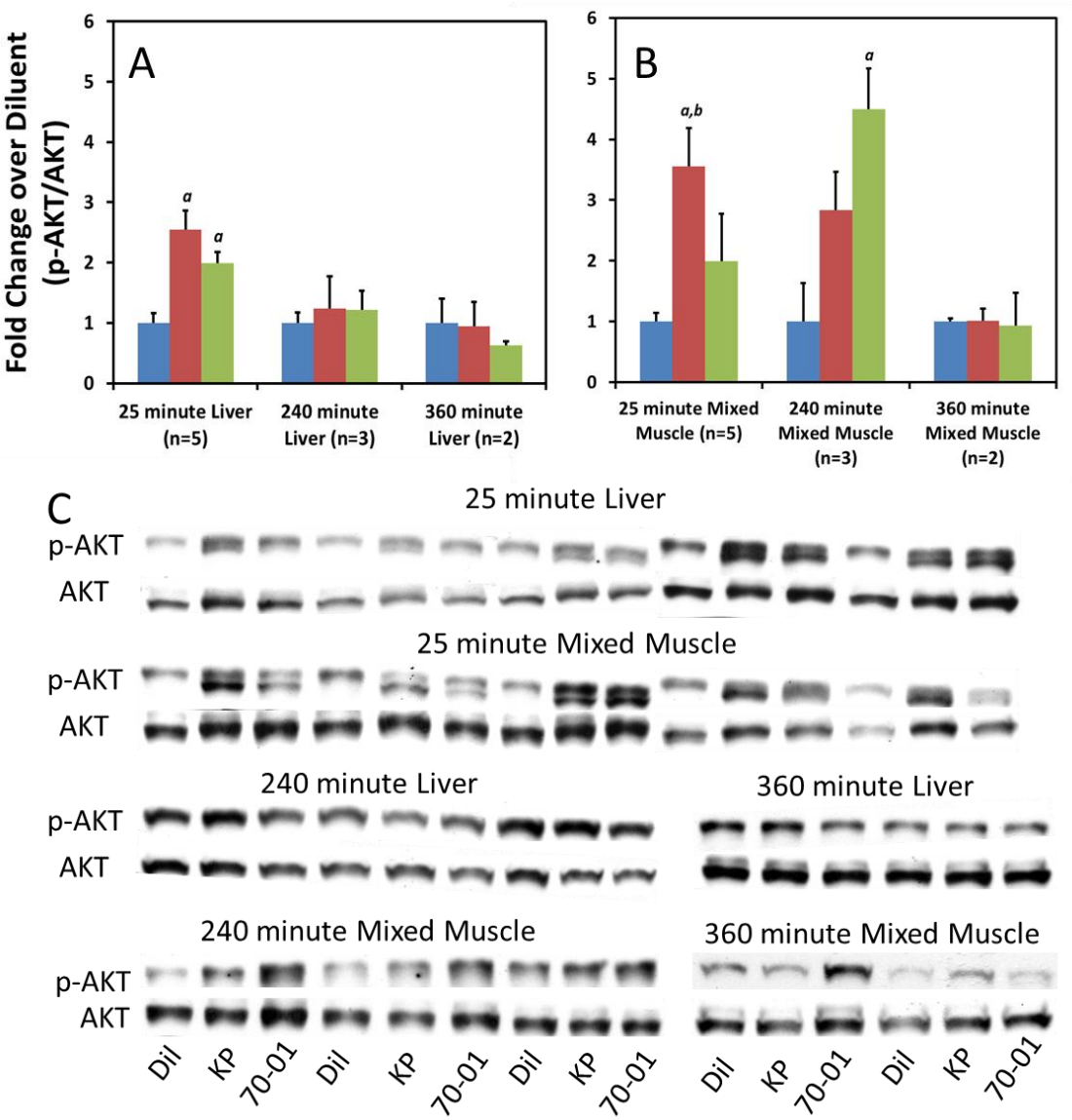

Fig 11. Effect of KP and 70-01 insulin on phosphorylation of AKT in the liver and mixed muscle at later time points. Western blot data representing the fold change over diluent of phosphorylated AKT in liver **(A)** and mixed muscle **(B)**. STZ-induced diabetic rats were injected subcutaneously with diluent (blue), or 3.07 nmol/ 300 gm body weight KP (red) or 70-01 (green) all in 100 µl diluent. Rats were sacrificed at 25 minutes, 240 minutes, or 360 minutes after injection and liver and mixed (quadriceps) muscle were harvested. N's are noted for each group; mean ± SE. ^{a} indicates $p < 0.05$ compared to diluent; ^{b} indicates $p < 0.05$ compared to 70-01. Actual western blots of the phosphorylated AKT **(C).**

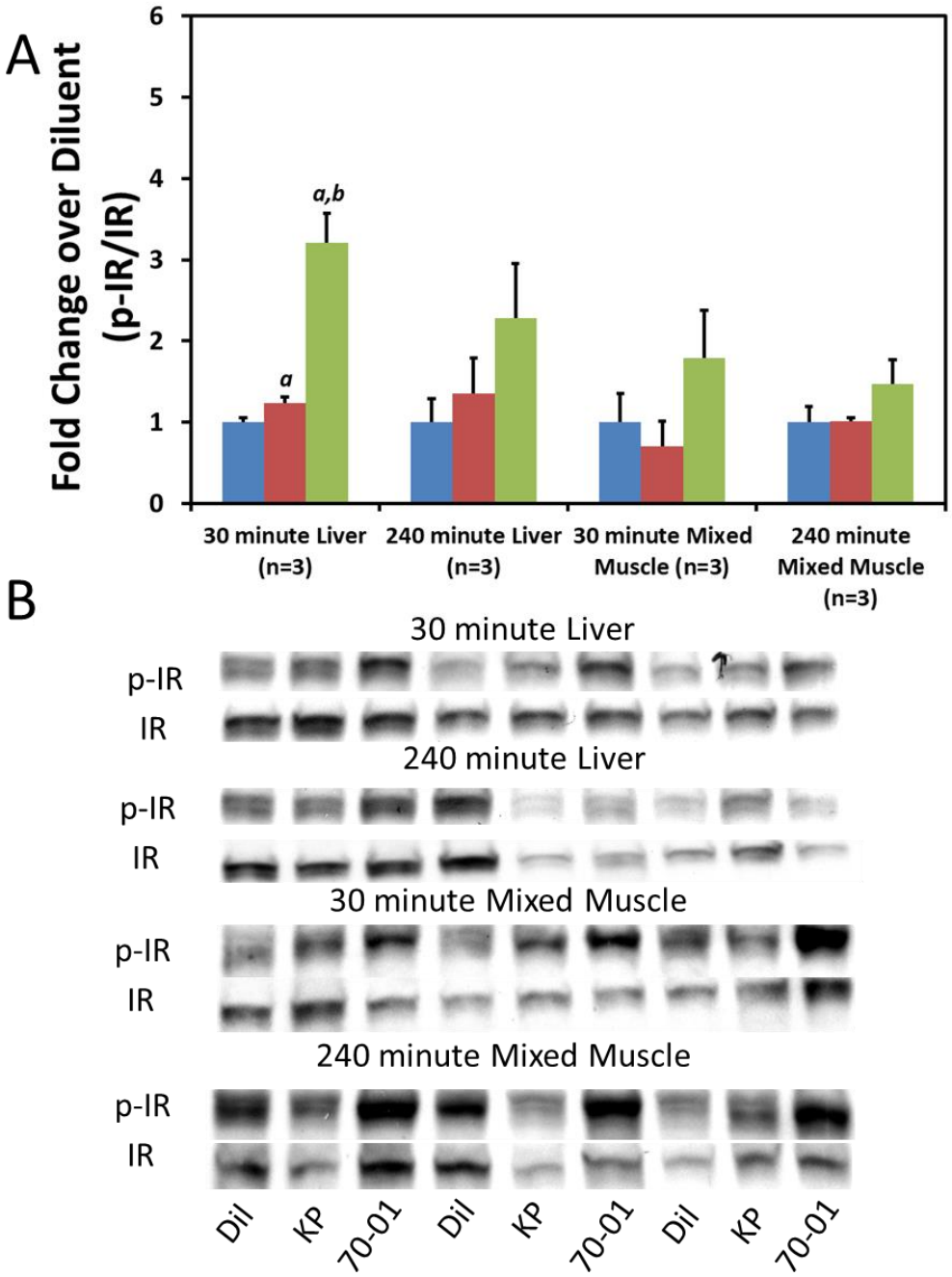

Fig 12. Effect of KP and 70-01 insulin on tyrosine phosphorylation of the insulin receptor in the liver and mixed muscle at later time point. Western blot data representing the fold change over diluent of tyrosine phosphorylated insulin receptor in liver and mixed muscle **(A)**. STZ-induced diabetic rats were injected subcutaneously with diluent (blue), or 3.07 nmol/ 300 gm body weight KP (red) or 70-01 (green) all in 100 µl diluent. Rats were sacrificed at 30 minutes, or 240 minutes after injection and liver and mixed (quadriceps) muscle were harvested. Mean ± SE. ^{a} indicates $p < 0.05$ compared to diluent; ^{b} indicates $p < 0.05$ compared to KP. Actual western blots of the phosphorylated insulin receptor **(B).**

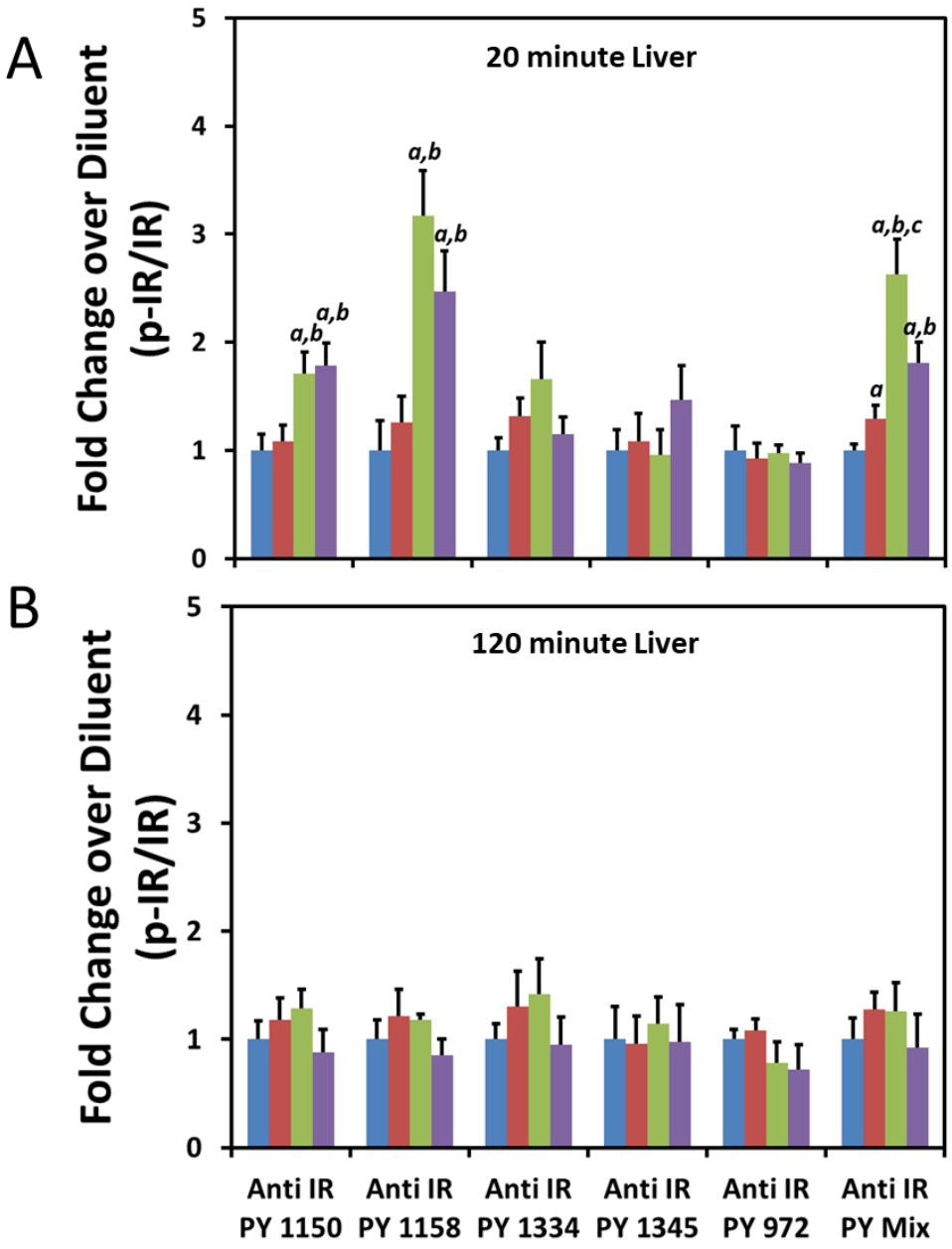

Fig 13. Effect of KP, 70-01, & 81-01 insulin on tyrosine phosphorylation of IR in liver tissue of the rat. Western blot data representing the fold change over diluent of different phosphorylated tyrosine residues on the insulin receptor. STZ-induced diabetic rats were injected with diluent (blue), or 2.56 nmol/ 300 gm body weight of KP (red), 70-01 (green) or 81-01 (purple) all in 100 µl diluent. Rats were sacrificed at either 20 minutes (**A**) or 120 minutes (**B**) and liver was harvested. n=6; [a] indicates $p < 0.05$ compared to diluent; [b] indicates $p < 0.05$ compared to KP; [c] indicates $p < 0.05$ compared to 81-01.

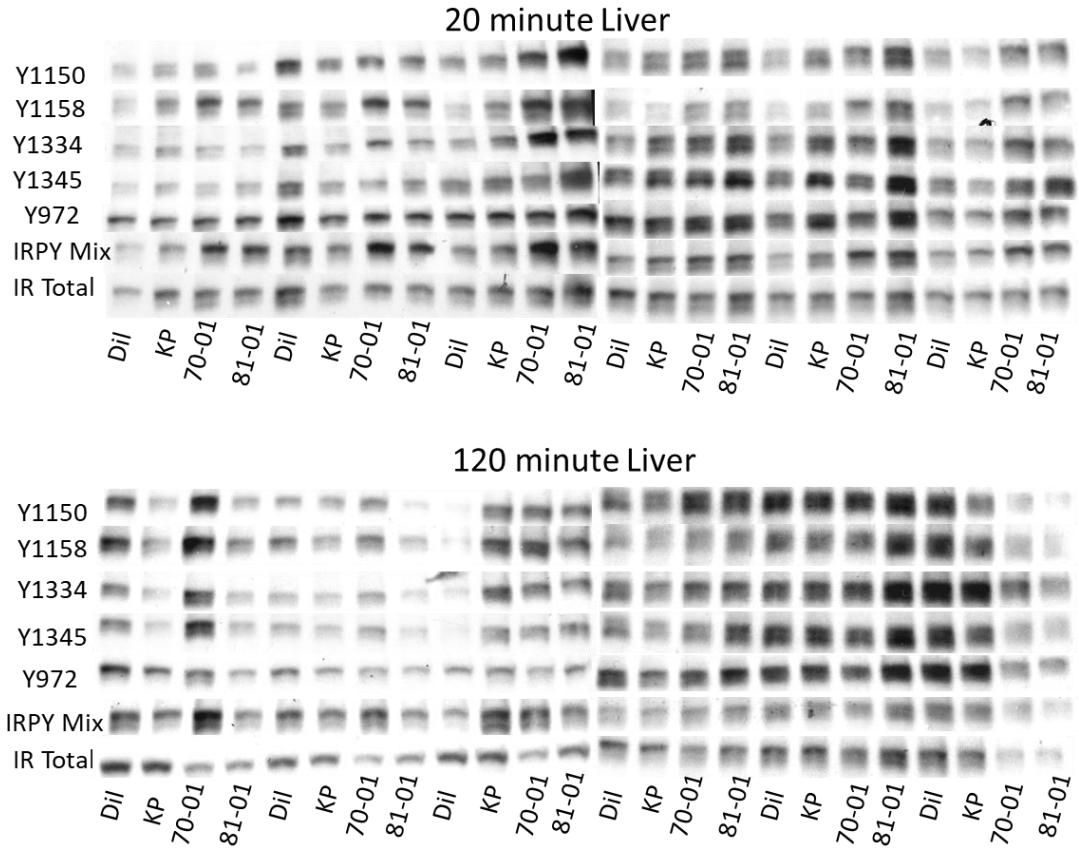

Fig 13-1. Western blots of phosphorylated tyrosine residues on the insulin receptor in liver tissue. IRPY mix is a mixture of all 5 phosphorylated tyrosine antibodies.

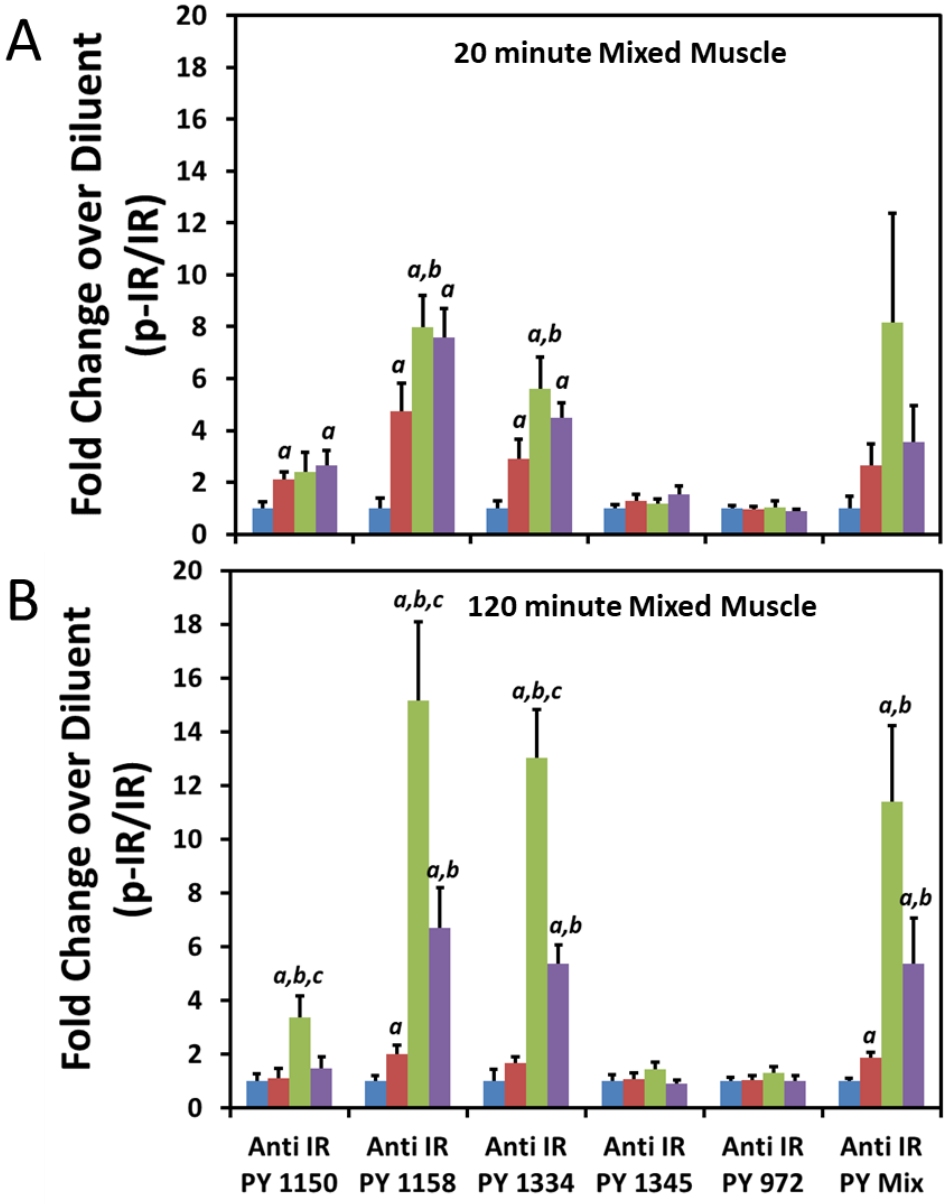

Fig 14. Effect of KP, 70-01, & 81-01 insulin on tyrosine phosphorylation of IR in mixed muscle tissue of the rat. Western blot data representing the fold change over diluent of different phosphorylated tyrosine residues on the insulin receptor. STZ-induced diabetic rats were injected with diluent (blue), or 2.56 nmol/ 300 gm body weight of KP (red), 70-01 (green) or 81-01 (purple) all in 100 µl diluent. Rats were sacrificed at either 20 minutes (**A**) or 120 minutes (**B**) and mixed muscle was harvested. n=6; ^{a} indicates $p < 0.05$ compared to diluent; ^{b} indicates $p < 0.05$ compared to KP; ^{c} indicates $p < 0.05$ compared to 81-01.

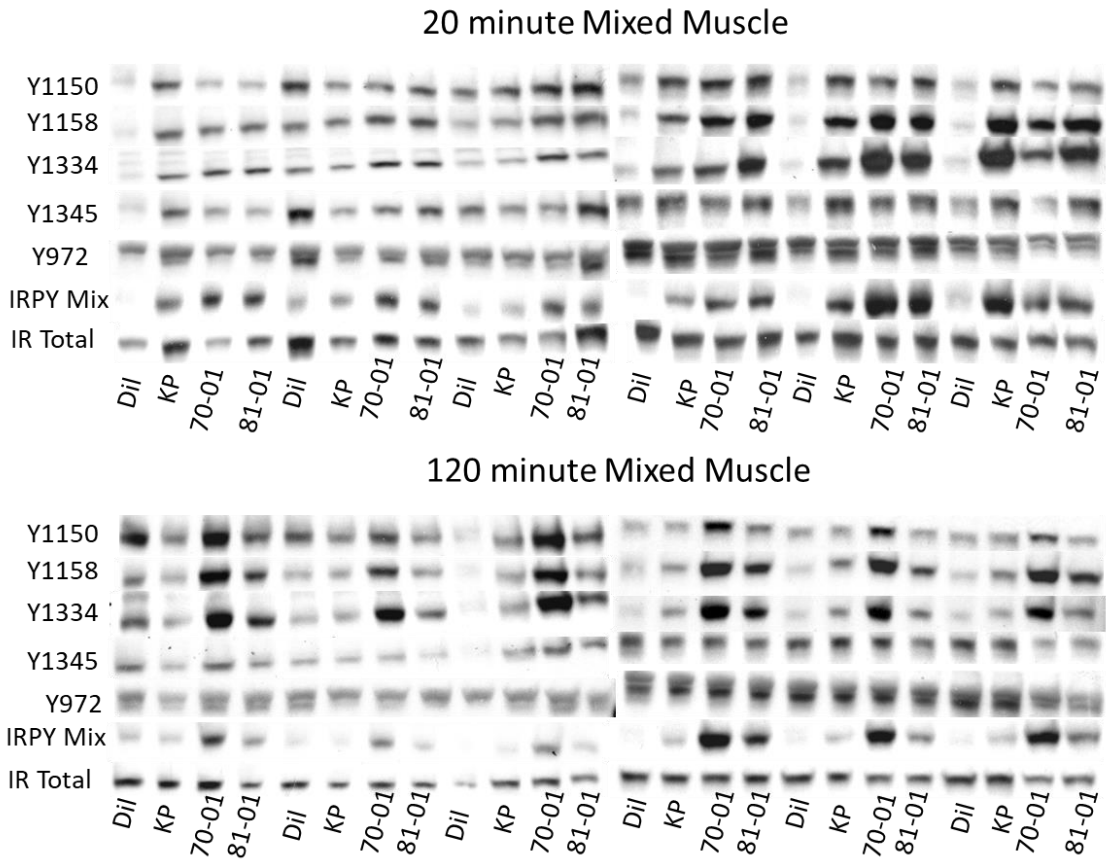

Fig 14-1. Western blots of phosphorylated tyrosine residues on the insulin receptor in mixed muscle tissue. IRPY mix is a mixture of all 5 phosphorylated tyrosine antibodies.

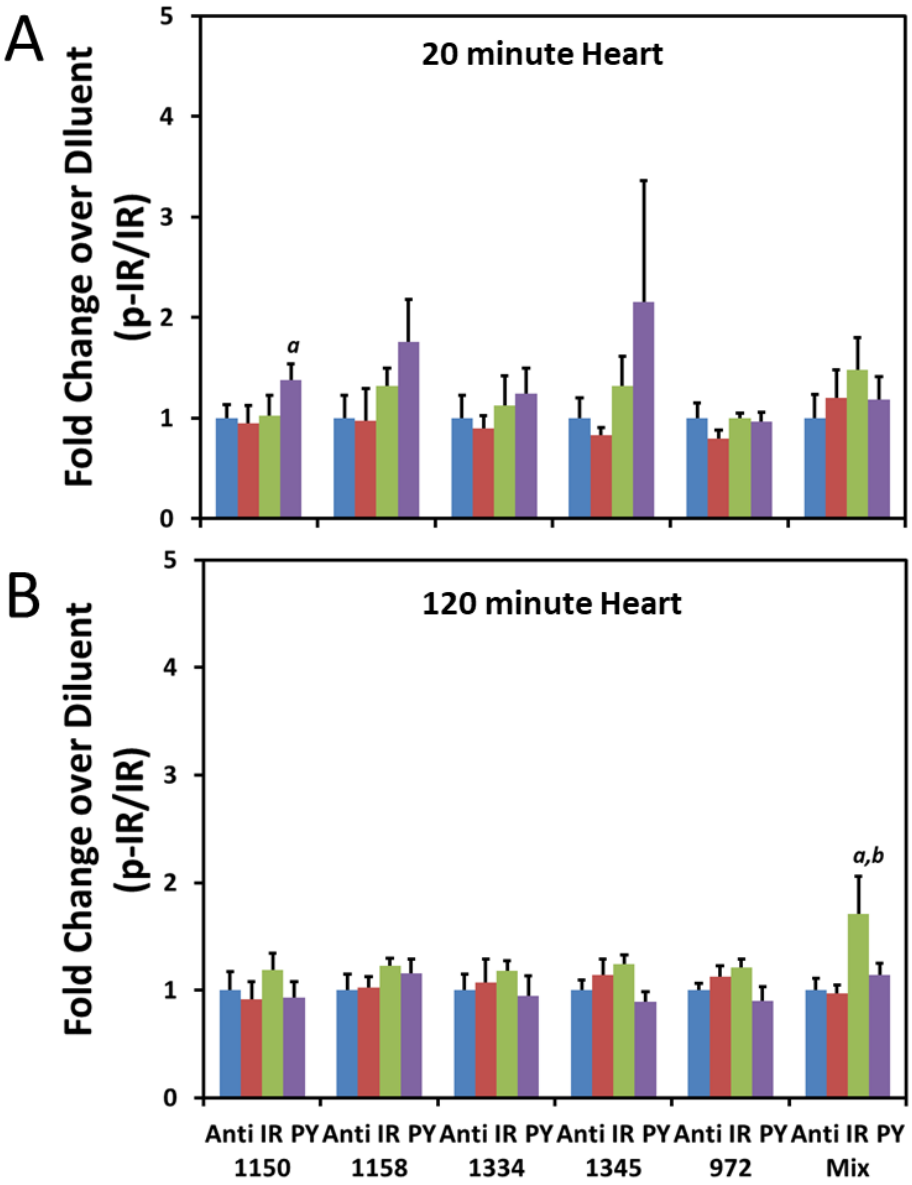

Fig 15. Effect of KP, 70-01, & 81-01 insulin on tyrosine phosphorylation of IR in heart tissue of the rat. Western blot data representing the fold change over diluent of different phosphorylated tyrosine residues on the insulin receptor. STZ-induced diabetic rats were injected with diluent (blue), or 2.56 nmol/ 300 gm body weight of KP (red), 70-01 (green) or 81-01 (purple) all in 100 µl diluent. Rats were sacrificed at either 20 minutes (**A**) or 120 minutes (**B**) and heart was harvested. n=6; ^{a} indicates $p < 0.05$ compared to diluent; ^{b} indicates $p < 0.05$ compared to KP.

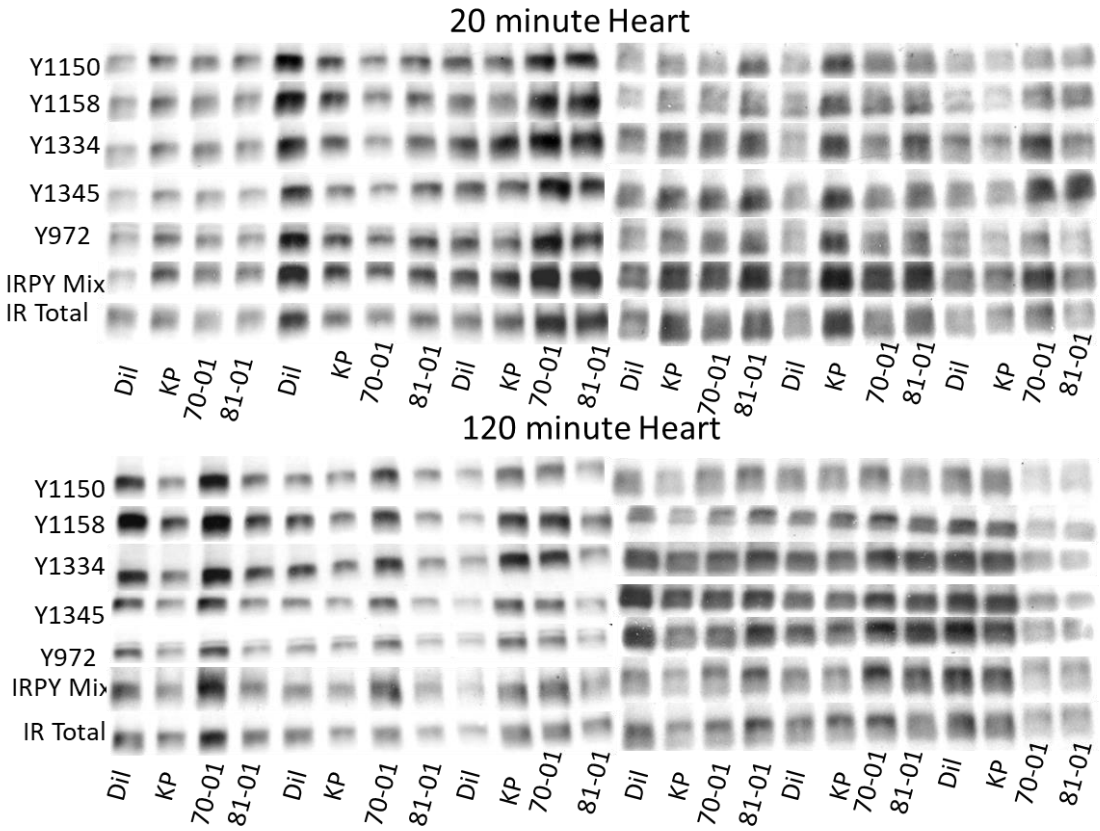

Fig 15-1. Western blots of phosphorylated tyrosine residues on the insulin receptor in heart tissue. IRPY mix is a mixture of all 5 phosphorylated tyrosine antibodies.

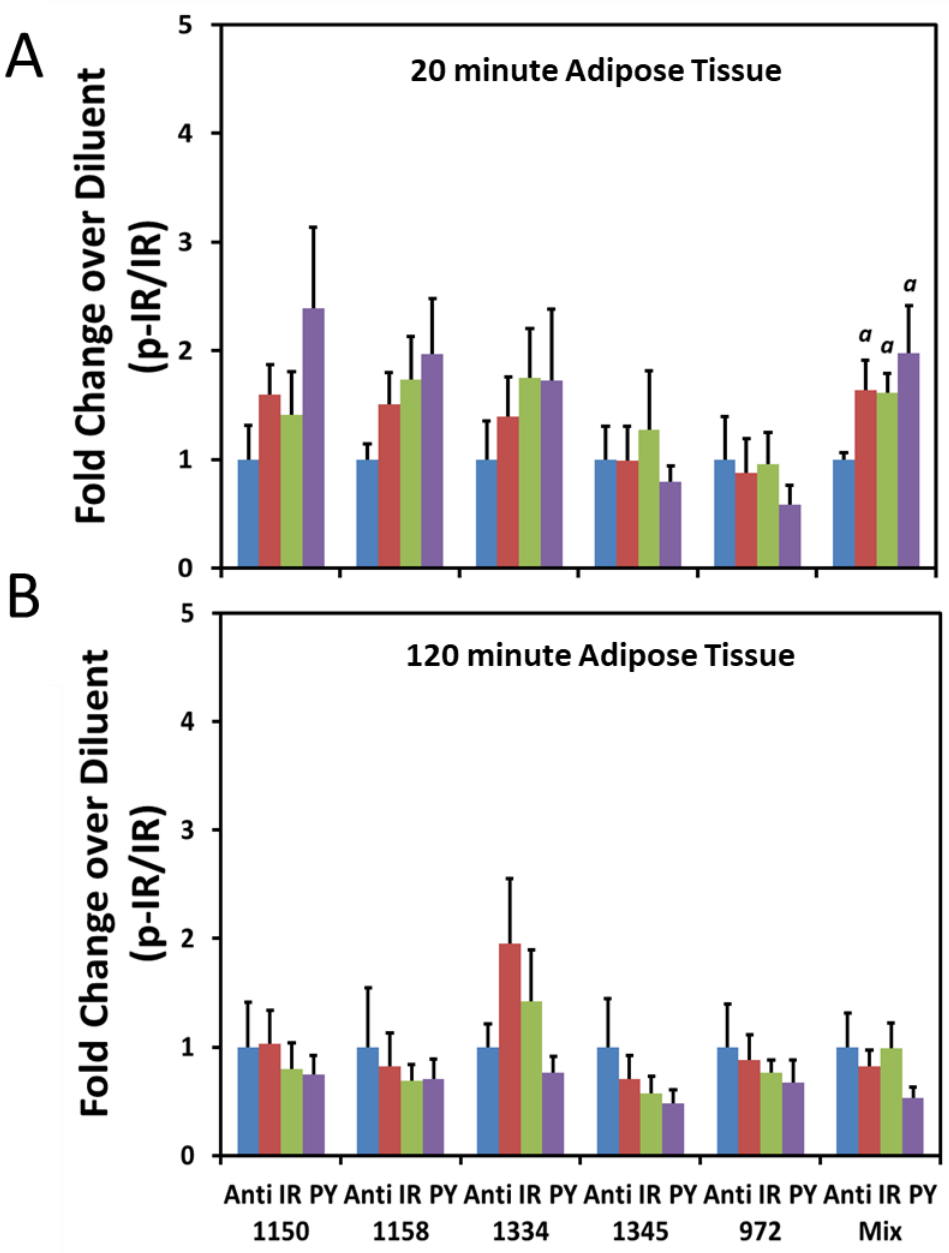

Fig 16. Effect of KP, 70-01, & 81-01 insulin on tyrosine phosphorylation of IR in adipose tissue of the rat. Western blot data representing the fold change over diluent of different phosphorylated tyrosine residues on the insulin receptor. STZ-induced diabetic rats were injected with diluent (blue), or 2.56 nmol/ 300 gm body weight of KP (red), 70-01 (green) or 81-01 (purple) all in 100 µl diluent. Rats were sacrificed at either 20 minutes (**A**) or 120 minutes (**B**) and adipose tissue was harvested. n=6; ^{a} indicates $p < 0.05$ compared to diluent.

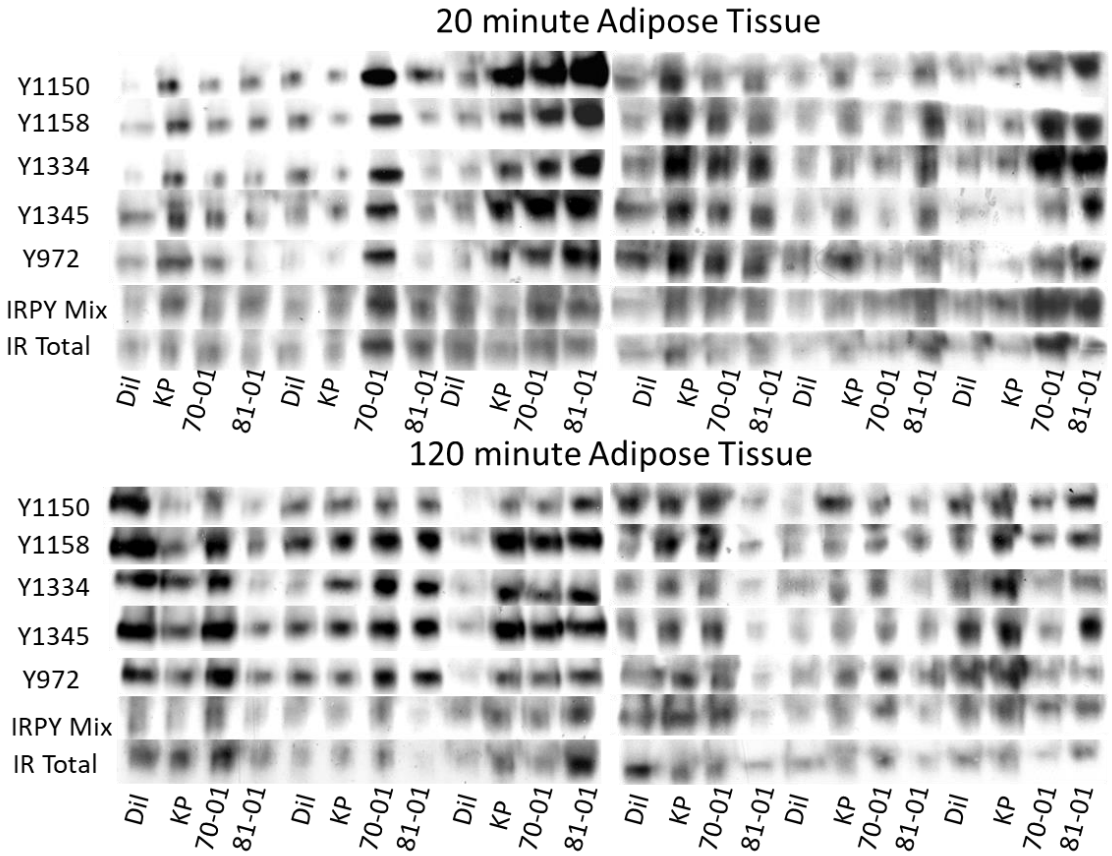

Fig 16-1. Western blots of phosphorylated tyrosine residues on the insulin receptor in adipose tissue. IRPY mix is a mixture of all 5 phosphorylated tyrosine antibodies.

References

1. Hua Q. Insulin: a small protein with a long journey. *Protein Cell.* 2010, 1:537-551.
2. White M. (2012). Mechanisms of insulin action. In J. Skyler (Ed.), *Atlas of diabetes: Fourth edition* (4th ed., pp. 19-38) Springer Science + Business Media, LLC.
3. Weiss M, Steiner D, & Philipson L. (2014). Insulin biosynthesis, secretion, structure, and structure-activity relationships. In L. De Groot, G. Chrousos, K. Dungan & a. et (Eds.), *Endotext [internet]* (pp. 1-45) South Dartmouth (MD).
4. Mayer JP, Zhang F, DiMarchi RD. Insulin Structure and Function. *Biopolymers (PeptideScience).* 2007, 88:687-713.
5. Ryle AP, Sanger F, Smith LF, Kitai R. The Disulphide Bonds of Insulin. *Biochem J.* 1955, 60:541-556.
6. Schaffer L. A model for insulin binding to the insulin receptor. *Eur. J. Biochem.* 1994, 221:1127-1132
7. Cieniewicz AM, Cooper PR, McGehee J, Lingham RB, Kihm AJ. Novel method demonstrates differential ligand activation and phosphatase-mediated deactivation of insulin receptor tyrosine-specific phosphorylation. *Cellular signaling.* 2016, 28:1037-1047.
8. Dorrestijn J, van Bussel FJ, Maassen JA, & Gomes de Mesquita DS. Early Steps in Insulin Action. *Archives of physiology and Biochemistry.* 1998, 106:269-289.
9. American Diabetes Association. Statistics about Diabetes. 2016. <http://www.diabetes.org/diabetes-basics/statistics/>

10. Gale EA. Insulin *lispro*: a new quick-acting insulin analogue. *Expert Opin Investig Drugs.* 1997, 6:1247-56.

11. Burge MR, Rassam AG, Schade DS. *Lispro* Insulin: Benefits and Limitations. *Trends in Endocrinology & Metabolism.* 1998, 9:337-41.

12. Hua Q, Nakagawa SH, Jia W, Huang K, Phillips NB, Hu S, Weiss MA. Design of an Ultrastable Single-chain insulin analogue: Synthesis, Structure, and Therapeutic Implications. *The Journal of Biological Chemistry.* 2008, 283:14703-16.

13. American Diabetes Association. Diagnosis and Classification of Diabetes Mellitus. *Diabetes Care.* Jan 2014, 37 (Supplement 1): S81-S90. <https://doi.org/10.2337/dc14-S081>.

14. Hansen BF, Danielsen GM, Drejer K, Sorensen AR, Wiberg FC, Klein HH, Lundemose AG. Sustained signaling from the insulin receptor after stimulation with insulin analogues exhibiting increased mitogenic potency. *Biochem J.* 1996, 315: 271-279.

15. Hamel FG, Siford GL, Fawcett J, Chance RE, Frank BH, Duckworth WC. Differences in the cellular processing of Asp^{B10} Human insulin compared with human insulin and Lys^{B28} Pro^{B29} Human insulin. *Metabolism.* 1999, 48: 611-617.

16. Phillips NB, Whittaker J, Ismail-Beigi F, Weiss MA. Insulin fibrillation and protein design: topological resistance of single-chain analogs to thermal degradation with application to a pump reservoir. *J Diabetes Sci Technol.* 2012, 6: 277-288.

17. Huang K, Maiti NC, Phillips NB, Carey PR, Weiss MA. Structure specific effects of protein topology on cross-beta assembly: studies of insulin fibrillation. *Biochemistry.* 2006, 45: 10278-93.
18. Hubbard SR. The Insulin Receptor: Both a Prototypical and Atypical Receptor Tyrosine Kinase. *Cold Spring Harb Perspect Biol.* 2013, 5: a008946.
19. Boucher J, Kleinridders A, Kahn CR. Insulin Receptor Signaling in Normal and Insulin-Resistant States. *Cold Spring Harb Perspect Biol*. 2014,µ 6:a009191.
20. (2006). *Glucose Clamping the Conscious Mouse: A Laboratory Course*. Vanderbilt-National Institute of Diabetes and Digestive and Kidney Diseases Mouse Metabolic Phenotyping Center, University of Vanderbilt, Nashville, Tennessee.
21. Bagg W, Plank LD, Gamble G, Drury PL, Sharpe N, Braatvedt GD. The effects of intensive glycaemic control on body composition in patients with type 2 diabetes. *Diabetes, Obesity, and Metabolism.* 2001, 3: 410-416.